

# Paleolimnology of a fluvial lake downstream of Lake Superior and the industrialized region of Sault Saint Marie

**Euan D. Reavie, John A. Robbins, Eugene F. Stoermer, Marianne S.V. Douglas, Gail E. Emmert, Nancy R. Morehead, and Alena Mudroch**

**Abstract:** A paleolimnological study was undertaken to describe the past environment of the St. Mary's River downstream of Lake Superior. Two sediment cores were obtained from the deepest part of Lake George, a fluvial lake in the river system. Rigorous analyses of radionuclides ( $^{210}\text{Pb}$ ,  $^{226}\text{Ra}$ , and  $^{137}\text{Cs}$ ) and chemical properties provided an accurate sediment chronology. More than 450 diatom species from 47 genera were identified. Diatom and geochemical data indicated gradual environmental change in response to anthropogenic activities, including logging, hydrologic manipulation, and steel, leather, and paper industries. A decline in water quality occurred gradually from the late 1800s through the 20th century in response to human activities, as was apparent from an increase in eutrophic-planktonic diatom taxa. A decline in benthic taxa and an increase in contaminant metals were also contemporaneous with impacts during the 20th century. Subfossil diatoms were similar to those recorded in paleolimnological investigations from the Great Lakes. However, diatom profiles indicate that the algal supply from upstream Lake Superior has been minimal and that the cores mainly reflect environmental characteristics of the near-upstream environment. Despite stochastic sedimentary regimes and complex habitats in the lotic system, this study reinforces the value of river paleolimnology at carefully selected sites.

**Résumé :** Nous avons entrepris une étude paléolimnologique afin de décrire les environnements du passé de la rivière St. Mary's en aval du lac Supérieur. Deux carottes de sédiments ont été prélevées du point le plus profond du lac George, un lac fluvial dans le réseau de la rivière. Des analyses précises des radionucléides ( $^{210}\text{Pb}$ ,  $^{226}\text{Ra}$  et  $^{137}\text{Cs}$ ) et des caractéristiques chimiques fournissent une chronologie exacte des sédiments. Plus de 450 espèces de diatomées appartenant à 47 genres ont pu être identifiées. Les diatomées et les données géochimiques indiquent un changement graduel du milieu en réaction aux activités humaines, en particulier, la coupe de bois, les manipulations hydrologiques et les industries du fer, du cuir et du papier. Il s'est produit un déclin graduel de la qualité de l'eau à partir de la fin des années 1800 et durant tout le 20<sup>e</sup> siècle en réaction aux activités humaines, comme le révèle l'augmentation des taxons de diatomées planctoniques à affinité eutrophe. Les impacts du 20<sup>e</sup> siècle se sont aussi accompagnés d'un déclin des taxons benthiques et d'une augmentation de la contamination par les métaux. Les diatomées subfossiles sont semblables à celles qui sont signalées dans les études paléolimnologiques dans les Grands Lacs. Cependant, les profils de diatomées indiquent que l'apport d'algues du lac Supérieur situé en amont est très faible et que les carottes reflètent surtout les caractéristiques environnementales du milieu immédiatement en amont. Malgré les régimes de sédimentation stochastiques et les habitats complexes du système fluvial, notre étude confirme la valeur des études paléolimnologiques dans les cours d'eau à des sites choisis avec soin.

[Traduit par la Rédaction]

Received 11 March 2004. Accepted 26 May 2005. Published on the NRC Research Press Web site at <http://cjfas.nrc.ca> on 19 October 2005.  
J18387

**E.D. Reavie.**<sup>1</sup> Center for Water and the Environment, Natural Resources Research Institute, 1900 East Camp Street, Ely, MN 55731, USA.

**J.A. Robbins and N.R. Morehead.** Great Lakes Environmental Research Laboratory, 2205 Commonwealth Boulevard, Ann Arbor, MI 48105-2945, USA.

**E.F. Stoermer.** School of Natural Resources, University of Michigan, 430 East University, Ann Arbor, MI 98109-1115, USA.

**M.S.V. Douglas.** Department of Geology, University of Toronto, 22 Russell Street, Toronto, ON M5S 3B1, Canada.

**G.E. Emmert.** The Cooperative Institute for Limnology and Environmental Research, University of Michigan, 2200 Bonisteel Boulevard, Ann Arbor, MI 48109-2099, USA.

**A. Mudroch.** Environment Canada, National Water Resources Institute, 867 Lakeshore Road, Burlington, ON L7R 4A6, Canada.

<sup>1</sup>Corresponding author (e-mail: [ereavie@nrri.umn.edu](mailto:ereavie@nrri.umn.edu)).

## Introduction

Water quality in the Laurentian Great Lakes has been impacted by various environmental changes that occurred following settlement of the region approximately 300 years ago, particularly during the late 19th and 20th centuries when the establishment of human populations was significant. Patterns of environmental changes related to human activities have been well established in studies of sediment cores from the Great Lakes (Stoermer et al. 1993), and characterization of recent human impacts is ongoing. As in the rest of the Great Lakes system, the rivers have been impacted since European settlers arrived in the region, but these impacts are only recently being understood.

Lakes tend to be relatively stable basins that accumulate reliable archives of environmental markers in their sedimentary records. Rivers, on the other hand, have been relatively little studied using paleolimnological techniques, primarily because the sedimentary basins of rivers are affected by variations in flow regimes, potentially providing chronological uncertainty in sedimentary records. The sedimentary record in fluvial systems can be highly variable (from temporal variations in sediment accumulation) or incomplete (e.g., from scouring events). Rigorous evaluations of temporal signals, such as the vertical sequence of isotope concentrations, organic–inorganic composition, and deposits from known historical events, are critical to validate such studies and confirm that paleolimnological studies of flowing ecosystems can be just as robust as those from more stable sedimentary basins. For example, Carignan et al. (1994) dated numerous sedimentary profiles from the St. Lawrence River, downstream of Lake Ontario, and further paleolimnological investigations were performed on the cores with consistent temporal records of sediment accumulation (Reavie et al. 1998).

Although unique paleoenvironmental trends have been identified in each of the Great Lakes, some broad-scale observations have been made. These include a long period of relatively stable fossil assemblages prior to European settlement, a very significant spike in nutrient loading associated with forest clearance, gradual escalation in productivity following settlement, increased changes in productivity and assemblage composition following land clearance and agricultural development throughout the 19th century, and dramatic increases in productivity during the 20th century (Stoermer et al. 1985a; Schelske et al. 1986). Some studies (Wolin et al. 1991; Schelske and Hodell 1995; Stoermer et al. 1996) suggest that, since the mid-1970s, there has been a water quality improvement partly as a result of rehabilitation efforts (the US–Canada Great Lakes Water Quality Agreement of 1972).

The current study considers the siliceous microfossil history of Lake George, a fluvial lake in the St. Mary's River system, downstream of Lake Superior. Previous paleolimnological investigations of this basin (Tenzer et al. 1999) indicated that some areas contain continuous (i.e., temporally complete) sedimentary records and that a relationship exists between human impacts and accumulation of sedimentary organic matter. In particular, organic matter accumulation increased dramatically during the 20th century in response to increased delivery from land-based anthropogenic sources,

providing preliminary evidence of the effects of European settlement. While some historical environmental data exist for the St. Mary's River (Upper Great Lakes Connecting Channels Study 1989; Kauss 1991), little monitoring was undertaken before the 1970s. Paleolimnological approaches, however, can be used to identify some of the chemical, physical, and biological changes that have occurred in the past.

The most commonly used biological indicators in paleolimnological analyses are diatoms (class Bacillariophyceae). Several studies exist concerning the taxonomy and environmental characteristics of river diatoms (e.g., Stevenson et al. 1996). However, diatom remains have rarely (e.g., Reavie et al. 1998) been used in paleoecological analyses of river sediment cores. Fluvial lakes provide unique opportunities to study lotic paleoenvironments, but the application of traditional paleolimnological methods to these rivers needs additional consideration.

Our intention was to study the paleoenvironmental trends in the St. Mary's River through an examination of sedimentary indicators. Our investigation had five major aims: (i) establish a recent and consistent sediment chronology using a combination of radioisotopic and chemical analyses, (ii) characterize the sedimentary diatom flora of Lake George and its upstream systems, (iii) relate paleoecological trends in the diatom flora to sedimentary chemical indicators of contamination and other human activities in the watershed, (iv) assess the effectiveness of a paleolimnological investigation in a lotic ecosystem, and (v) compare the paleolimnology of the St. Mary's River with that from other regions in the Laurentian Great Lakes.

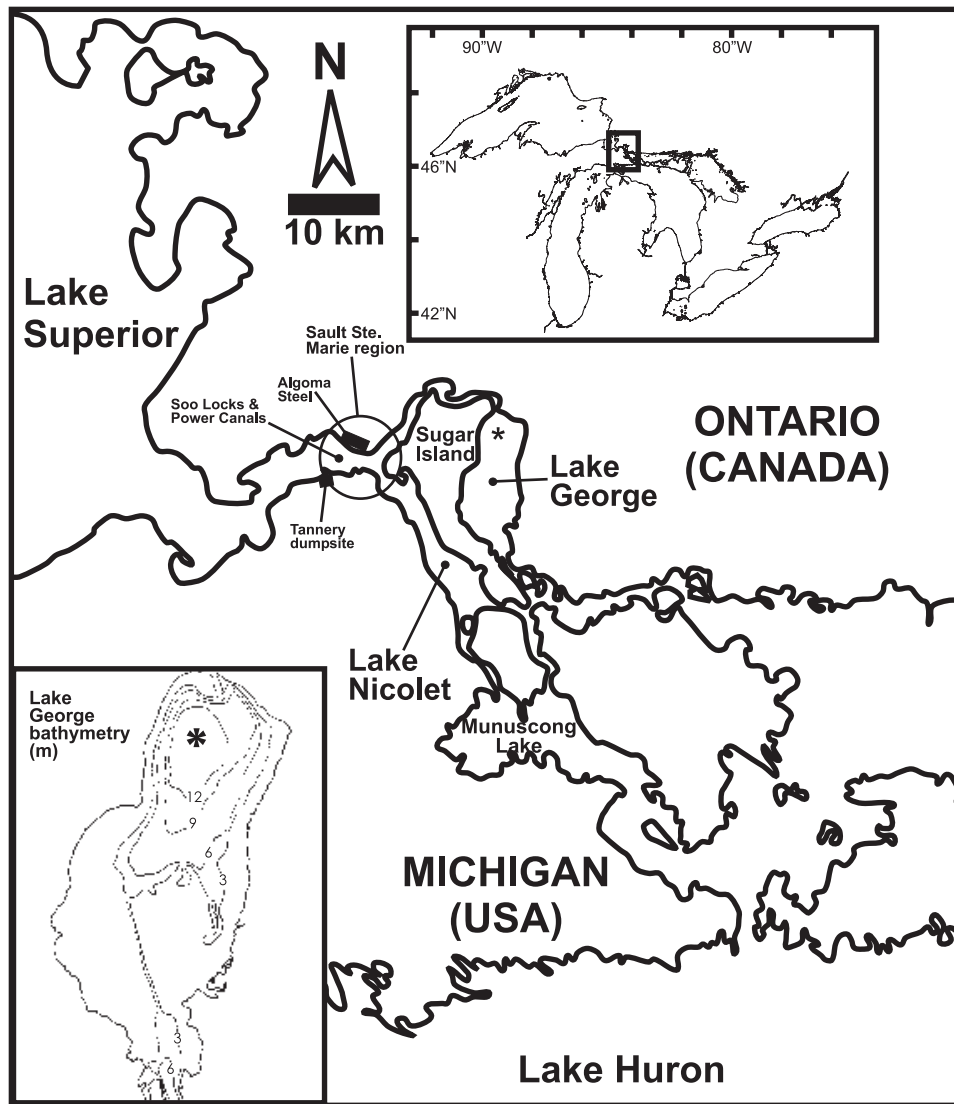
## Materials and methods

### Study site

The St. Mary's River is a 112-km connecting channel between Lakes Superior and Huron (Fig. 1). Just downstream of Lake Superior, the river passes by the heavily industrialized twin cities of Sault Saint Marie (Ontario and Michigan) and then divides, where about 30% of the water supply passes through the fluvial Lake George on its way to Lake Huron (Liston et al. 1986). Water passing rapidly through the narrow north channel flows over a sill as it enters Lake George and spreads out over a 15-m-deep bathymetric feature (Tenzer et al. 1999) that is a remnant glacial plunge pool. This feature, which makes up the northern third of the lake, is where particle loads settle and accumulate at high rates (up to about 0.5 cm·year<sup>-1</sup>). About 95% of the water entering Lake George comes from Lake Superior, with the remaining 5% coming from local streams and rivers. Hydraulically, the St. Mary's River is a fast-response system. On average, a parcel of water passing through the Sault Locks arrives at Lake George within a couple of days and is flushed out within 1 week. Lake George's watershed area is approximately 2200 km<sup>2</sup>. Although this watershed contributes only about 5% of the water flow to Lake George, it contributes a relatively high fraction (about 90%) of the total sediment load.

Prior to European settlement, this region was an Algonkian Indian Nation. The first nonnative visited in 1618, and the area later became established as a center for social, cul-

**Fig. 1.** Map of Lake George (Ontario, Canada) and surrounding region (the upper inset shows location in Great Lakes region). An asterisk indicates the sediment coring site.



tural, and economic activity (Newton 1976). In 1783, the North West Fur Trading Company founded a post and built a narrow canal to bypass the rapids on the St. Mary's River. Construction of the more substantial canal, which still exists today, began in 1888 and was completed in 1855. Between 1870 and 1880, the native forests in the river catchment were largely cleared, which increased soil erosion and leaching of soil nutrients. For a few decades, residents then engaged mainly in lumbering and subsistence farming. Although logging persisted from the 1850s through the 1940s in Michigan's Upper Peninsula (Karamanski 1989), the late 1800s represented the most important logging period in Lake George's watershed. The greatest industrial development in the river catchment and the river occurred in the 20th century, and the river is now well known for severe impairment of water quality, sediment (Nichols et al. 1991), and biota (Kauss 1991) as a result of major point and nonpoint industrial and agricultural discharges (Hamdy et al. 1978). Some of the contaminants of concern have included oils and greases, suspended solids, metals, nutrients, bacteria, and

polycyclic aromatic hydrocarbons (Upper Great Lakes Connecting Channels Study 1989). Sources of contamination have included the steel industry (i.e., Algoma Steel), two Ontario water pollution control plants, the pulp and paper industry (i.e., St. Mary's Paper), tanning agents from the Northwestern Leather Company, one Michigan wastewater treatment plant, and upstream sources along Ontario tributaries. Continued urban and industrial development and operation of navigational structures are also a concern for the quality of the river.

#### Coring

Two sediment cores from Lake George were investigated in this study. The primary core was obtained in fall 1993 at a 13-m-deep site (46°29.4'N, 86°7.5'W) located within the area of maximum sediment deposition (Fig. 1). Sediments were retrieved using a modified Soutar box corer that provided undisturbed material with excellent interface preservation. A subcore ~50 cm in length was obtained by slow insertion of a 10-cm-diameter polycarbonate tube into the

box core sample. To extend the paleochronology, we used samples from deep sections of a secondary, 72-cm-long core collected in summer 1986 (Tenzer et al. 1999) at essentially the same site (within a horizontal distance of 50 m). This core was obtained for the Upper Great Lakes Connecting Channel study (Upper Great Lakes Connecting Channels Study 1989) by a SCUBA diver using a 2.73-cm-diameter polybutyrate tube. Sediments in both cores, extruded from tubes on site and sliced into 1- or 2-cm-thick sections, were stored frozen in precleaned polyethylene bottles for return to the laboratory.

### Radionuclide analysis

Activities of the uranium-series radionuclides  $^{226}\text{Ra}$  ( $t_{1/2} = 1600$  years) and  $^{210}\text{Pb}$  ( $t_{1/2} = 22.3$  years), and anthropogenic  $^{137}\text{Cs}$  ( $t_{1/2} = 30.2$  years) were determined using a combination of two independent nuclear measurement techniques: gamma spectroscopy to obtain true total activities of  $^{210}\text{Pb}$ ,  $^{226}\text{Ra}$ , and  $^{137}\text{Cs}$  and alpha spectroscopy to maximize precision in specifying activities of acid peroxide extracted  $^{210}\text{Pb}$ .

For the gamma method,  $4.00 \pm 0.01$  g of freeze-dried, disaggregated sediment was packed in polypropylene tubes to a standardized geometry, sealed to allow for in-growth of radon progeny, and then counted using a high-resolution HpGe well detector calibrated by standards whose accuracy and precision were determined using US National Institute of Standards and Technology (NIST) or British Calibration Service (BCS) certified standards. Gamma standards were prepared either by doping aliquots of whole dry sediments from Lake George with standard solutions or by counting NIST sediment gamma standards. Standard solutions included a BCS-calibrated Amersham-Searle mixed radionuclide standard QCY.46 and a NIST standard solution SRM 4233B for  $^{137}\text{Cs}$ , a NIST-calibrated solution obtained from the US Environmental Protection Agency (Las Vegas, Nevada) for  $^{210}\text{Pb}$ , and solution SRM 4959 for  $^{226}\text{Ra}$ . This standard was prepared in 1967 for distribution as a 2.00- $\mu\text{g}$ , initially  $^{210}\text{Pb}$ -free solution stored in ampoules. Because of precisely quantifiable  $^{210}\text{Pb}$  in-growth over many years, the solution could be also used for independent calibration of  $^{210}\text{Pb}$ . Several additional NIST sediment standards were used primarily for  $^{137}\text{Cs}$ : SRM 4305B river sediment, SRM 4353 Rocky Flats soil, and SRM 4354 freshwater lake sediment. Activity of  $^{210}\text{Pb}$  was determined from the direct 46.5-keV gamma emission,  $^{226}\text{Ra}$  from gamma emissions of progeny,  $^{214}\text{Pb}$  at 295.2 and 351.9 keV, and  $^{214}\text{Bi}$  at 603.9 keV, and  $^{137}\text{Cs}$  from the 661.6-keV emission.

For the alpha method, we determined the activity of a decay product,  $^{210}\text{Po}$  ( $t_{1/2} = 138$  days), in secular equilibrium with  $^{210}\text{Pb}$  (Flynn 1968). A calibrated amount of  $^{209}\text{Po}$  ( $t_{1/2} = 100$  years) was added to  $2.00 \pm 0.001$  g of dry sediment and then treated using a mixture of 50% HCl with periodic additions of 30% hydrogen peroxide. The two isotopes of polonium self-plated onto polished copper disks placed in the extracts. Exposed disks were counted using high-resolution surface barrier alpha detectors. The  $^{209}\text{Po}$  solution was calibrated by coplating precisely known amounts of this solution and a NIST standard solution of  $^{208}\text{Po}$  (SRM 4327).

Mean analytical errors for total  $^{210}\text{Pb}$ ,  $^{226}\text{Ra}$ ,  $^{137}\text{Cs}$ , and acid peroxide extractable (AP)  $^{210}\text{Pb}$  are expressed as coefficients of variation (CV =  $100 \times \text{SD}/\text{mean}$ ) in percent  $\pm$

values that measure their downcore variability about the mean. Within the upper 20 cm, CVs average  $7.2 \pm 2.3$ ,  $5.8 \pm 2.0$ ,  $2.6 \pm 1.0$ , and  $2.6 \pm 0.2$ , respectively. Below 20 cm, corresponding values are  $24 \pm 15$ ,  $6.6 \pm 1.0$ , not detected, and  $3.8 \pm 0.6$ . Thus, even in the upper sections of core where  $^{210}\text{Pb}$  is relatively well determined, the precision is almost three times better for AP  $^{210}\text{Pb}$ .

### Calculation of the supported fraction of AP $^{210}\text{Pb}$

Because of the superior precision of the alpha counting method, core dating is based on AP  $^{210}\text{Pb}$ . Sediment extracts consist of a mixture of excess  $^{210}\text{Pb}$  plus an amount incompletely leached from mineral components containing radium. In the present study, there are two ways to determine background contributions: (i) rigorously by codetermination of total  $^{210}\text{Pb}$  and  $^{226}\text{Ra}$  and (ii) to obtain an average value by extrapolation of AP  $^{210}\text{Pb}$  activity profiles to core depths where excess  $^{210}\text{Pb}$  is negligible.

The distribution of total  $^{210}\text{Pb}$  is given by

$$(1) \quad A_{T\gamma}(g) = A_{E\gamma}(g) + A_{R\gamma}(g)$$

where  $A_{E\gamma}$  is the specific activity of excess  $^{210}\text{Pb}$  ( $\text{dpm}\cdot\text{g}^{-1}$ ; 1 dpm = 60 Bq),  $A_{R\gamma}$  is the specific activity of  $^{226}\text{Ra}$  ( $\text{dpm}\cdot\text{g}^{-1}$ ), and  $g$  is the cumulative dry weight of sediment at core section midpoints ( $\text{g}\cdot\text{cm}^{-2}$ ). Mass rather than linear units are used as a measure of depth in determining core section ages to eliminate effects of water exclusion. However, profile data are displayed in linear units. The distribution of AP  $^{210}\text{Pb}$  is

$$(2) \quad A_{T\alpha}(g) = A_{E\alpha}(g) + f_m A_{R\gamma}(g)$$

where  $f_m$  is the matrix extraction efficiency. Since both methods recover all excess  $^{210}\text{Pb}$ ,  $A_{E\gamma} = f_c A_{E\alpha}$ , where  $f_c$  is an intercalibration factor (ideally equal to 1.0). Hence, it can be seen from eqs. 1 and 2 that

$$(3) \quad A_{T\gamma}(g) = f_c A_{T\alpha}(g) + (1 - f_c f_m) A_{R\gamma}(g)$$

A least-squares optimized fit using eq. 3 and data for the entire length of core yields values of  $f_c(\text{opt})$  and  $f_m(\text{opt})$ . The AP  $^{210}\text{Pb}$  distribution is then

$$(4) \quad A_{T\alpha}(g) = A_{E\alpha}(g) + f_m(\text{opt}) A_{R\gamma}(g)$$

where the second term (a product) is the depth-dependent background.

Alternatively, in the present case where AP  $^{210}\text{Pb}$  decreases exponentially from some depth to the core bottom, the distribution is

$$(5) \quad A_{T\alpha}(g) = A_{E\alpha}(0) e^{-\lambda t} + A_s$$

where  $\lambda$  is the radioactive decay constant ( $= 0.69315/t_{1/2} = 0.03114\cdot\text{year}^{-1}$ ),  $r_s$  is the net mass accumulation rate ( $\text{g}\cdot\text{cm}^{-2}\cdot\text{year}^{-1}$ ),  $A_{E\alpha}(0)$  is the surface activity ( $\text{dpm}\cdot\text{g}^{-1}$ ),  $t = g/r_s$ , and  $A_s$  is supported activity of AP  $^{210}\text{Pb}$ . Least-squares optimized fit of eq. 5 to data yields values of  $r_s(\text{opt})$  and  $A_s(\text{opt})$ . The optimized value of  $A_{E\alpha}(0)$  does not properly estimate surface activity unless the AP  $^{210}\text{Pb}$  distribution is exponential for the entire core length. Optimized values are used for extrapolation of age–depth assignments. For eqs. 3 and 5, optimized parameters were determined with the Levenberg Marquardt method (Press et al. 1989).



### Calculation of mean ages of core sections from mappings

For tracer-based chronologies to be valid, there must be no significant mixing of sediments, no discontinuities in accumulation rates such as might occur for episodic erosion or deposition, and no redistribution of tracer either by bio-transport or by interstitial diffusion. When these conditions are met, a profile of AP  $^{210}\text{Pb}$  is given by

$$(6) \quad A_{\text{E}\alpha}(g) = [F_s(t)/r_s(t)]e^{-\lambda t}$$

where  $F_s$  is the rate of supply of excess  $^{210}\text{Pb}$  (disintegrations per minute per square centimetre per year) and  $t$  is the age of sediment at depth  $g$ . This equation is the basis for three alternative mapping algorithms or point transformations (Robbins and Herche 1993): CRS (constant rate of supply), which assumes that  $F_s$  is constant but allows for a variable  $r_s$ , CRA (constant rate of accumulation), which assumes that  $r_s$  is constant but allows for a variable  $F_s$ , and CIA (constant initial activity), which assumes that  $F_s$  and  $r_s$  covary so that the ratio  $[F_s(t)/r_s(t) = A_{\text{E}\alpha}(0)]$  remains constant. Note that eq. 6 reduces to the first term in eq. 5 when  $r_s$  and  $F_s$  are both constant.

Mathematical expressions for the three alternative age-depth mappings are developed and discussed in detail elsewhere (Robbins and Herche 1993). Briefly, age-depth relationships for the CRA and CIA algorithms are  $t(g) = g/r_s$  and  $t(g) = -(1/\lambda)\ln[A_e(g)/A_e(0)]$ , respectively. It can be shown that for CRS,  $t(g) = -(1/\lambda)\ln[1 - S(g)/S(\infty)]$  and  $r_s(g) = [S(\infty) - S(g)]/[\lambda A_{\text{E}\alpha}(g)]$ , where  $S(g)$  is the integral of excess  $^{210}\text{Pb}$  activity from the surface to depth  $g$ . For each of the three mappings, CRA, CIA, and CRS, least-squares optimized values of parameters held constant are, respectively,  $r_s = 0.150 \pm 0.01 \text{ g}\cdot\text{cm}^{-2}\cdot\text{year}^{-1}$ ,  $A_e(0) = 15.0 \pm 0.4 \text{ dpm}\cdot\text{g}^{-1}$ , and  $F_s = \lambda S(\infty) = 3.43 \pm 0.03 \text{ dpm}\cdot\text{cm}^{-2}\cdot\text{year}^{-1}$ . Standard deviations associated with ages and mass accumulation rates reflect analytical errors propagated by Monte Carlo methods (Press et al. 1989) and represent minimum uncertainties.

### Element analysis

#### Determination of element concentrations

Total concentrations of 25 trace elements (Al, As, Br, Ca, Ce, Co, Cr, Cs, Eu, Fe, Hf, La, Lu, Mn, Na, Rb, Sb, Sc, Sm, Ta, Th, Ti, V, Yb, and Zn) were determined by instrumental neutron activation analysis (Alfassi 1998). Dry sediment samples (200 mg) together with sediment standards were irradiated with thermal neutrons. For the 1986 core, standards used were US Geological Survey andesite AGV-1 and granite G-2 (Flanagan 1973, 1974; Govindaraju 1994). For the 1993 core, we used the NIST SRM 1633a coal fly ash standard in addition to AGV-1 and G-2. Gamma rays from activated samples were counted on a high-resolution solid-state detector and multichannel analyzer system and the resultant spectra were processed to quantify concentrations of selected elements. For additional details, see Dams and Robbins (1970). Average precisions (as CVs) in determining concentrations of elements listed above were, respectively, 4%, 7%, 5%, 7%, 4%, 3%, 9%, 6%, 6%, 1%, 5%, 6%, 14%, 3%, 1%, 12%, 13%, 5%, 5%, 14%, 3%, 11%, 5%, 10%, and 4%. Concentrations of an additional three elements (Cd, Cu, and Pb with CV = 5% in all cases) were determined by flame atomic absorption spectrophotometry using acid peroxide extracts of dry sediment (10% HCl by volume with

periodic additions of hydrogen peroxide) and Fisher standard solutions (Rossmann 1995). Concentrations of total carbon (TC, CV = 3%), inorganic carbon (IOC, CV = 20%), and total nitrogen (TN, CV = 5%) were determined using a Perkin Elmer Series 2400 CHN analyzer calibrated with acetanilide. For IOC analysis, 60 mg samples were analyzed on an Oceanography International carbon analyzer by evolution of  $\text{CO}_2$  from samples treated with 5 mL of 10%  $\text{H}_3\text{PO}_4$ . Gas was allowed to evolve for several minutes prior to its introduction into the analyzer. To insure complete collection of evolved gas, each treated sample was repeatedly analyzed to capture additional gas released, and final values were reported as the sum of successive measurements. Large errors in determination of IOC reflect concentrations close to detection limits. Total phosphorus (TP) (CV = 5%) was determined by the ignition method (Anderson 1976; Murphy and Riley 1962).

Finally, concentrations of biogenic silica (BSi) (CV = 5%) were determined by treatment of about 30 mg of sediment with 0.2 mol  $\text{NaOH}\cdot\text{L}^{-1}$  to dissolve silica followed by neutralization of extracts with 0.5 mol  $\text{H}_2\text{SO}_4\cdot\text{L}^{-1}$  (Krause et al. 1983) and analysis of the filtered extract for silicon by the molybdate blue method using a Technicon autoanalyzer calibrated with Fisher standard solutions. We first analyzed sediment (1986 core, 15–16 cm depth) by sequential extraction. Three capped plastic test tubes with replicate sediment and extractant were placed in a shaker bath with water at 93.9 °C. At nine nominal times (1.5, 5, 10, 20, 30, 60, 75, 90, and 120 min) from the start of extraction, aliquots of the hot sample were withdrawn from test tubes by syringe. The extraction process was immediately arrested by adding acid and rapidly cooling. The sequential extraction procedure was also undertaken for 1986 core sediments at depths of 38–39 cm (15 times over 2.5 h) and 68–70 cm (8 times over 2 h). For each of the three core sections, increases in the amount of silicon extracted corresponded to a combination of fast and slow reactions, which were graphically analyzed to estimate BSi concentrations from the fast reaction component. The results showed that a fixed 20-min extraction time, suggested by Krause et al. (1983), produced values of BSi that were consistent with timed extraction values. Thus, to reduce analytical effort, we adopted a 20-min fixed time for analysis of the remaining core samples.

#### Interelement associations

To identify groups of elements with similar downcore trends, a factor analysis was performed on 61 observations of downcore concentrations for each of 32 elements using the proprietary program PROSTAT (version 3.01) (Poly Software International, Pearl River, New York). Starting with a correlation matrix derived from linear regression between element pairs, the program provided factor loadings, which were constrained to the first four factors that ranked highest in percentage of explained variance (totaling ~70%). The remaining variance explained (30%) was distributed over a large set of components for which no meaning could be identified.

#### Construction of an element-based contamination index

A subset of nine elements (As, Cr, Cu, Fe, Mn, Pb, TC, TP, and Zn) that are contaminants associated principally with the industrial and postindustrial periods were used to

construct a generalized measure of the degree of river contamination downstream from Sault Saint Marie. The contamination index  $C_{\text{ndx}}(t)$  was calculated as the average of background-subtracted, peak-normalized concentrations of the above elements. That is, for the  $i$ th element with concentration  $C_i(t)$ ,  $C_{\text{ndx}}(i,t) = [C_i(t) - C_i(\text{bg})]/[C_i(\text{max}) - C_i(\text{bg})]$ , where the background concentration  $C_i(\text{bg})$  is taken as the concentration in the deepest core section and  $C_i(\text{max})$  is the maximum concentration. The  $C_{\text{ndx}}(t)$  is the average of nine values of  $C_{\text{ndx}}(i,t)$  for each core section with mean age  $t$ .

### Microfossil preparations

For siliceous microfossil analyses, a 1-g subsample of freeze-dried sediment was placed in a 20-mL glass vial and digested with a mixture of concentrated nitric and sulfuric acid (1:1 by volume). The samples were heated at  $\sim 100^\circ\text{C}$  in a water bath for 1 h. Samples were rinsed with distilled water until no acid remained and siliceous remains were plated on coverslips using the quantitative Battarbee (1986) method. Cover slips were mounted on slides using Naphrax<sup>®</sup> medium. For each slide, diatom valves were identified using oil immersion on a Leica DMRB microscope (1000 $\times$  magnification). Siliceous specimens were identified along a transect until at least 500 diatom valves were enumerated. Diatoms were identified to the species level or higher using standard floras (e.g., Krammer and Lange-Bertalot 1986–1991; Patrick and Reimer 1966) and iconographs (Camburn et al. 1984–1986; Cumming et al. 1995; Reavie and Smol 1998). Fragments of diatom valves were enumerated and combined with the valve sum when possible. Other siliceous remains (i.e., phytoliths, sponge spicules, chrysophyte scales and stomatocysts, and the plates of testate amoebae) were also enumerated. These entities were generally rare, and only chrysophyte remains were sufficiently abundant to be considered further.

### Zone determination

A cluster analysis was performed on the relative abundances of common taxa (occurred in at least two samples with at least 2% abundance in one or more samples). A total of 62 taxa were included in this analysis. Cluster analysis to define zones of similar assemblages was implemented with the computer program CONISS in conjunction with the computer program TILIA using the Euclidean distance measure (Carney 1982). Cluster analysis was depth constrained to maintain clusters within uninterrupted depth ranges. To clarify changes in diatom assemblages downcore, zones were derived based on the Euclidean distance between the various arms in the cluster analysis. The significance of these zones was determined using Bennett's (2002) software program PSIMPOLL 4.10, which includes an option for testing zones using the broken-stick model (Bennett 1996). The broken-stick model identifies zonations with variances considered to be interpretable by exceeding values generated by a random distribution of zones. This testing was used to confirm the level of zonation that was interpretable, based on the amount of variation in the diatom data accounted for in each zonation step, and so allowed us to effectively determine the strongest periods of ecological transition in Lake George's paleolimnological diatom record.

### Multivariate statistical analyses

Because the zonation method described above is constrained by depth, the extracted relationships between diatom assemblages and pollution variables are limited to specific zones or time periods. To identify taxonomic specificity to downcore environmental measurements, principal patterns in the distributions of diatom taxa relative to sedimentary chemistry data were explored using canonical correspondence analysis (CCA).

Ordinations were performed on diatom relative abundance and chemical data using CANOCO version 4.5 (ter Braak and Šmilauer 2002). A preliminary detrended correspondence analysis was used to determine the maximum amount of variation in the species data (Hill and Gauch 1980), also called the species gradient. This gradient, if greater than 4 SD units, reflects the unimodal distribution of species in the data set, thereby warranting the use of unimodal methods (i.e., CCA) in further analyses (ter Braak and Šmilauer 2002).

CCA was used to explore the relationships among distributions of diatom taxa and the sedimentary chemical variables. The same common taxa used in cluster analysis were included in the CCA. Environmental variables were progressively selected using forward selection based on the amount of variation in the diatom data explained by each variable.

## Results and discussion

### Sediment chronology

Assignments of ages to core section depths are based on determination of excess AP  $^{210}\text{Pb}$ , defined as the difference between total activities of AP  $^{210}\text{Pb}$  and a background supplied by in situ decay of  $^{226}\text{Ra}$ . The excess  $^{210}\text{Pb}$  method, first used by Goldberg (1993), is now widely employed and has been discussed in detail by Robbins (1978), Appleby and Oldfield (1992), and Robbins and Herche (1993).

There are two potentially significant difficulties in establishing sediment chronologies for Lake George. First, there is the intrinsic problem that sediments of the lake and St. Mary's River historically have been populated by a variety of organisms that can mix sediments (Burt et al. 1991). It is not possible to determine the extent and possible effects of sediment mixing from our data. We note that for a long period of record, sediments were sufficiently contaminated to suppress populations of benthic invertebrates, and we rely on the internal consistency of our interpretation of results to support a conclusion that sediment mixing at the site has not been significant. Second, there is the methodological problem that the rate of supply of excess  $^{210}\text{Pb}$  to sediments may not have been constant. Common to nearly all published computational approaches to  $^{210}\text{Pb}$  dating is the assumption of constant rate of supply. Our remedy is to apply three alternative computational methods (CRS, CRA, and CIA) for establishing  $^{210}\text{Pb}$ -based age–depth assignments and to test the ability of each method to account for marker dates based on indicator elements ( $^{137}\text{Cs}$ , Cr, and Fe) where features of their profiles (markers) can be associated with known dates of historical events. Recently, Smith (2001) suggested that  $^{210}\text{Pb}$  dating must be verified using at least one independent marker. In this paper, we go well beyond this minimal prescription for establishing the verity of chronological results.

### Background AP $^{210}\text{Pb}$

The primary use of the gamma data is to determine the activity and downcore variability of radium-supported background AP  $^{210}\text{Pb}$ . In the 1993 core, total activities of  $^{210}\text{Pb}$  (Fig. 2a, solid squares) decrease with depth to background levels approximating  $^{226}\text{Ra}$  beyond about 35 cm (Fig. 2a, open squares). Over the length of core,  $^{226}\text{Ra}$  averages  $1.93 \pm 0.24 \text{ dpm}\cdot\text{g}^{-1}$ . A linear regression of  $^{226}\text{Ra}$  activity versus cumulative weight gives an intercept of  $2.02 \pm 0.06 \text{ dpm}\cdot\text{g}^{-1}$  and marginally significant slope of  $-0.008 \pm 0.005 \text{ (dpm}\cdot\text{g}^{-1})/(\text{g}\cdot\text{cm}^{-2})$  ( $r = 0.25$ ,  $\text{df} = 48$ ,  $P < 0.1$ ).

The activity profile of total AP  $^{210}\text{Pb}$  (Fig. 2b) fluctuates considerably above 20 cm depth, but at greater depths, it decreases approximately exponentially with depth. Comparison of total  $^{210}\text{Pb}$  and  $^{226}\text{Ra}$  profiles (gamma analysis) with AP  $^{210}\text{Pb}$  (alpha analysis) using eq. 3 yields the optimized intercalibration factor  $f_c(\text{opt}) = 0.95 \pm 0.03$  and supported  $^{210}\text{Pb}$  extraction efficiency  $f_m(\text{opt}) = 0.81 \pm 0.09$ . The profile of total  $^{210}\text{Pb}$ , predicted by eq. 4 ( $r = 0.98$ ,  $P < 0.001$ ,  $n = 50$ ) is shown in Fig. 2a. Profiles of gamma- and alpha-determined specific activities of  $^{210}\text{Pb}$  are consistent if small differences in calibration and matrix extraction efficiencies are taken into account. According to eq. 4, the mean background ( $0.81 \times A_{R\gamma}(\text{g})$ ) is  $1.56 \pm 0.2 \text{ dpm}\cdot\text{g}^{-1}$ . Alternatively, using eq. 6, we obtain an excellent fit (Fig 2b, solid line) with  $r_s(\text{opt}) = 0.150 \pm 0.01 \text{ g}\cdot\text{cm}^{-2}\cdot\text{year}^{-1}$  and a mean background  $A_s(\text{opt}) = 1.37 \pm 0.1 \text{ dpm}\cdot\text{g}^{-1}$  ( $r = 0.994$ ,  $P < 0.001$ ,  $n = 30$ ). We have adopted this latter value, since it is better determined and establishes an asymptotic activity most consistent with use of AP  $^{210}\text{Pb}$ . The success of eq. 6 in accounting for the profile below 20 cm, using a constant value of  $r_s(\text{opt})$ , supports the validity of extrapolating sediment ages to depths beyond the reach of present core dating methods.

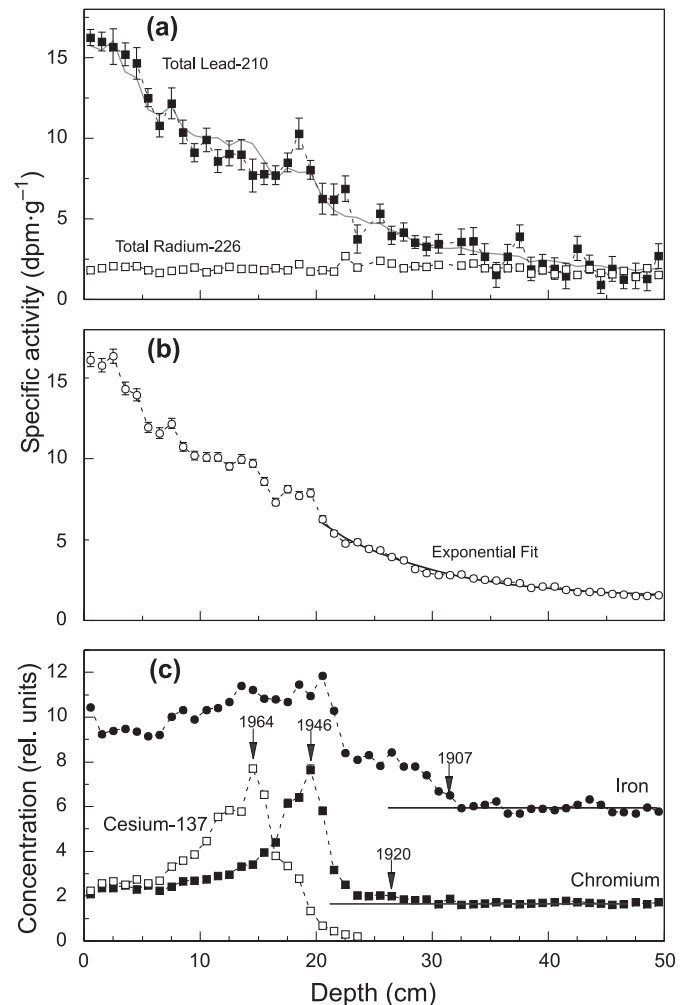
### Appending 1986 core data

Since the 1986 core is 22 cm longer than the 1993 core, it was possible to extend the taxonomic results back about 80 years by analyzing deep sections of the earlier core. The extension was straightforward because the profile of excess  $^{210}\text{Pb}$  in the 1986 core was also exponential below 20 cm depth, and  $r_s$ , derived using eq. 6, was  $0.145 \pm 0.005 \text{ g}\cdot\text{cm}^{-2}\cdot\text{year}^{-1}$  ( $r = 0.996$ ,  $n = 36$ ) and thus essentially the same as the 1993 core value. Hence, correct weights of 11 (2-cm) sections to be appended to the 1993 core could be determined by calculating the factor (1.049) by which the corresponding section weights in the 1986 core should be multiplied to maximize overlap between distributions of excess  $^{210}\text{Pb}$  at depths from 20 to 50 cm. The resulting extended distribution of excess  $^{210}\text{Pb}$  down to 50 cm is  $A_{T\alpha}(\text{g}) - 1.37$  as described above. Beyond that depth, they were calculated from eq. 6 using the indicated least-squares determined parameters. Element concentrations in attached core sections consist of corresponding concentrations in the 1986 core that have been multiplied by element-specific factors close to  $1.00 \pm 0.05$ , which optimize the overlap with 1993 core values.

### Establishing marker dates

Two principal stratigraphic features of the observed  $^{137}\text{Cs}$  profile are the peak at 14.5 cm depth and threshold at about 25 cm (Fig. 2c). This radionuclide is commonly used to sup-

**Fig. 2.** (a) Profiles of total  $^{210}\text{Pb}$  (solid squares) and  $^{226}\text{Ra}$  (open squares) in the 1993 core. The solid line is the profile of total  $^{210}\text{Pb}$  predicted by AP  $^{210}\text{Pb}$  using eq. 3. (b) Profile of AP  $^{210}\text{Pb}$ . The solid line is the least-squares optimized exponential fit (for depths  $>20$  cm) using eq. 5. (c) Depth profiles of temporal indicator elements. For ease of presentation, the concentrations were multiplied by arbitrary coefficients; the actual values are presented in other figures. Horizontal lines indicate background concentrations, and date assignments are shown based on known historical information about the elements.



port the validity sediment age assignments based on  $^{210}\text{Pb}$ . See Ritchie and Ritchie (2003) for a comprehensive bibliography on the use of  $^{137}\text{Cs}$  in studies of soil erosion and sediment accumulation. Significant global dispersal of  $^{137}\text{Cs}$  commenced with aboveground testing of thermonuclear weapons in 1952. Atmospheric testing effectively ended after October 1963 when the Limited Test Ban Treaty was implemented (Carter and Moghissi 1977). In the Great Lakes region, maximum deposition occurred in the spring of 1963 (Robbins 1985a). It has been shown (Robbins et al. 2000) that Cs peaks in sediments can be displaced forward by as much as 2 years as a result of time-averaging processes occurring on a system-wide scale. Thus, we consider the date of the peak marker and its uncertainty to be 1964 ( $-0.5 + 1.0$  years). The assignment of time to the threshold is more difficult, since it depends on arrival time of the signal at a



**Table 1.** Comparison of selected section age assignments based on profile features and historical data with various computational results for the 1993 core.

Profile feature	Depth (cm)	Established	Mean age (years)		
			CRS	CRA	CIA
<sup>137</sup> Cs peak	14.5	1964 -0.5, +1	1962±1	1951±3	1975±1
<sup>137</sup> Cs horizon	25.5	1952 -0, +1	1926±3	1918±5	1942±2
Cr peak	19.5	1946±3	1946±2	1935±4	1967±2
Cr horizon	26.5	1920±5	1923±3	1899±6	1937±2
Fe horizon	31.5	1907±3	1907±6	1895±7	1919±3

**Note:** CRS, constant rate of supply; CRA, constant rate of accumulation; CIA, constant initial activity.

coring site, as well as the sensitivity of analytical methods. We have somewhat arbitrarily made the assignment as 1952 (-0 + 2 years).

The profile of Cr (Fig. 2c) also has two stratigraphic features for which we can associate dates, the peak at 20.5 cm and a threshold at 26.5 cm. For many years, Lake George received significant loadings of this element from operations of the now defunct Northwestern Leather Company (Tannery) that was situated near the shore of St. Mary's River in Sault Saint Marie, Michigan. The company was founded in 1900 and, according to anecdotal reports (Tannery 1983), used extracts (tannic acid) from hemlock bark for tanning animal hides during the early part of the 20th century. Such plants as the Tannery made it possible for logging companies to profit from bark that they had previously discarded and, for a time, "spawned an entire subsidiary industry for the region" (Karamanski 1989). By the 1920s, hemlock bark harvesting had ended. We estimate from this and anecdotal reports that the switch from use of natural tannins to Cr salts must have occurred sometime between 1915 and 1925, ~1920 ± 5 years. This date is assigned to the depth (26.5 cm) where the concentration of Cr first rises significantly (>3 σ) above background levels.

For most of its 30-year post-tannin history, the company discharged Cr-laden materials directly into the St. Mary's River and dumped solid wastes containing Cr onto an 8-acre (1 acre = 0.404 ha) marshy area adjacent to the river. Company fortunes rose during World War II. In August 1947, a special study of river bottom deposits by the Michigan Department of Health (International Joint Commission 1951) showed that Ashmun Bay was seriously polluted by discharges from the Tannery waste. Water in the bay, located 3 km downstream from the company outfall, was turbid and contained numerous floating balls of hair, while "chrome wastes...colored the sand of the bay, but this waste was not noticeable in the river proper" (International Joint Commission 1951). However, the study also noted that contaminants generated by the Tannery (notably hairballs) on the US side of the river were found in the Lake George Channel and concluded that pollutants discharged to the river from both US and Canadian sides are subject to rapid cross-boundary mixing. While historical records of Cr discharge are likely nonexistent and indirect measures of output, such annual leather production or company income, are not accessible, the Tannery filed annual reports with the State of Michigan from 1929 to 1957 that provide year-end cash on hand (COH) data (Treasury 1929–1957). We think that COH is a measure of the level of collective human effort in production of tanned leather products and is likely strongly related to

the company's total annual Cr waste load. In 1938, COH was in the \$7000 range (corrected to 1950 dollars). During the short period from 1939 through 1946, COH rose to \$115 000 and then increased only slightly from 1947 through 1949 to its maximum of \$128 000. From 1950 onward, COH dropped precipitously to a low in 1957 of \$11 000. In 1958, the Tannery ceased operations. From these considerations, we estimate that peak Cr discharge occurred sometime between the middle of the war effort (1943) and the time of maximum COH (1949), or 1946 ± 3 years.

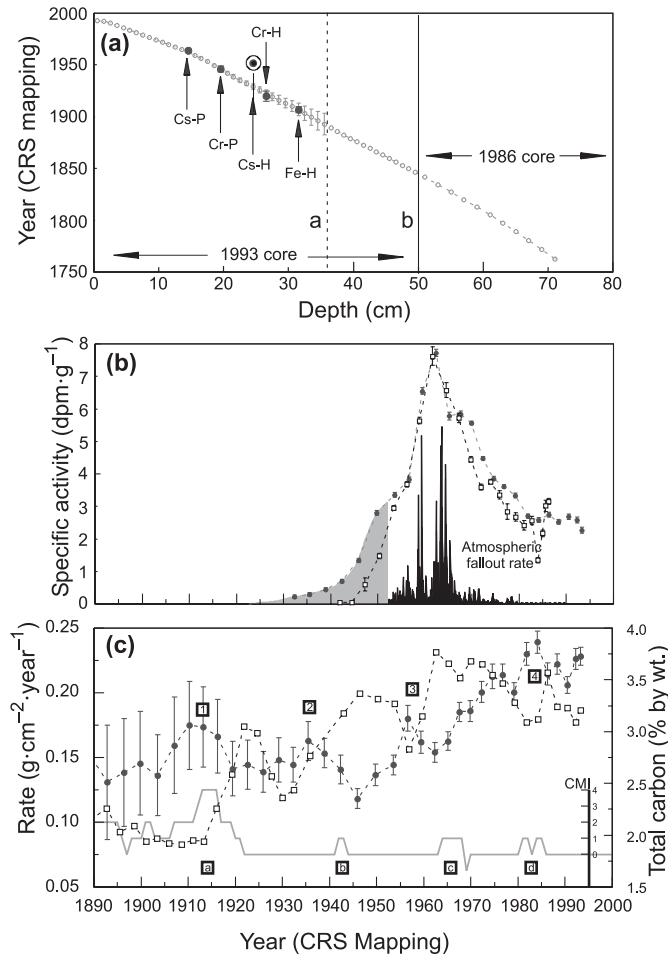
The profile of Fe (Fig. 2c) also has a stratigraphic feature for which we can associate a date, the rise at 31.5 cm. Sedimentary Fe concentrations are significantly elevated in this core as a result of the operations of the Algoma Steel Corporation. The company was founded as an ironworks in 1901 and commenced rolling steel rails in February 1902 according to a company report (April 2003) of its early history. By December of the same year, the company was forced to close because of lack of orders and as a result produced no rails in 1903. In the following year, control of the company was transferred to the Lake Superior Corporation, and subsequently, the Ontario and Canadian governments intervened to regulate the industry and meet payroll. We are uncertain about the importance of the company's output of iron and steel or associated loading of Fe to the St. Mary's river following transfer of ownership. However, their steel making operations were sufficiently viable by 1909 that the company acquired its own source of high-quality limestone, Fiborn Quarry in Mackinac County, Michigan (Michigan Karst Conservancy 2003). Thus, we assign a date as 1907 ± 3 years to the depth (31.5 cm) at which Fe concentrations are first significantly (±3 σ) greater than background.

#### Age–depth relationships

Compared with established ages, assignments (Table 1) based on CRA and CIA algorithms are consistently too early or too recent, respectively, for four out of the five independent age markers: <sup>137</sup>Cs and Cr peaks and Cr and Fe thresholds. For CRS, the agreement is excellent for these markers (Fig. 3a, solid circles). The CRS age–depth relationship for the extended core (Fig. 3a) is divided into three sections. The part from core surface to vertical line *a* denotes the limit that we have somewhat arbitrarily selected at 36 cm depth (1890) to terminate CRS age assignments. At this depth, the uncertainty in CRS age is about 12%, while the corresponding uncertainty in accumulation rate is about 36%. The middle section between lines *a* and *b*, 36–50 cm, denotes the region where ages have been assigned assuming a constant



**Fig. 3.** (a) Constant rate of supply (CRS) based age–depth relationship. Arrows indicate positions of independently established indicator element ages based on peak (P) and horizon (H) features. The questionable  $^{137}\text{Cs}$  horizon location (Cs-H) is encircled. (b) Specific activity of  $^{137}\text{Cs}$  versus CRS year for cores collected in 1986 (squares) and 1993 (circles), with estimated monthly fallout  $^{137}\text{Cs}$  to the lake shown as a histogram in relative units. The shaded tail indicates activity occurring below the expected  $^{137}\text{Cs}$  horizon. (c) Mass accumulation rate (circles) and total carbon (squares) versus CRS year. The CMI index indicates the number of major construction, maintenance, or improvement activities occurring at sites in the St. Mary's River upstream of Lake George.



sediment accumulation rate. Within the third region beyond line *b*, the age–depth relationship is further extrapolated to appended sections of the 1986 core.

#### The $^{137}\text{Cs}$ threshold problem

All three mapping algorithms considerably overestimate the age of the  $^{137}\text{Cs}$  threshold because the radionuclide has migrated downward. The CRS assigned age, 1926, is about 30 years too old (Fig. 3a, encircled point). It is beyond the scope of this study to discuss the reasons in detail. We offer the following observations and two alternative explanations for them: (i) limited biological or sampling induced mixing of sediments or (ii) diffusive mobility owing to compromised ability of sediments to bind  $^{137}\text{Cs}$ .

The success of CRS age assignments, apart from the  $^{137}\text{Cs}$  threshold, suggests that sediments have not been subject to much physical or biological mixing. However, temporal distributions of  $^{137}\text{Cs}$  for the 1986 and 1993 cores (Fig. 3b) are much broader than the fallout record (histogram) for the Great Lakes region (Robbins 1985a). Sediment profiles of  $^{137}\text{Cs}$  in the Great Lakes and elsewhere are often broader because atmospheric inputs are time averaged in sedimentary reservoirs prior to incorporation into permanent deposits (Robbins 1985b; Robbins et al. 2000, 2004). As a consequence of time averaging, activities remain elevated well after the cessation of new inputs. Overall, the distribution in the 1986 core is slightly narrower than in the 1993 core, while the most pronounced distribution difference occurs along the trailing edge (shaded area). This cannot be the result of predepositional time averaging of  $^{137}\text{Cs}$  in external reservoirs.

While the penetration and variable displacements could at least in part be ascribed to core-to-core variability, radiocesium strongly bound to particles could penetrate into pre-fallout sediments by biological mixing of limited extent or by coring (in 1986) or box subcoring (in 1993), simply as a result of downward smearing of material along the interface between a sediment core and the core tube. Such translocation would presumably increase threshold depths for Cr and Fe, but to a lesser extent, since these elements (unlike  $^{137}\text{Cs}$ ) have significant backgrounds.

An alternative explanation that we favour is that a small but significant fraction of  $^{137}\text{Cs}$  may be able to migrate in sediments. Under normal circumstances, in the Great Lakes, this radionuclide is bound strongly to expandable lattice clay minerals such as illite (Evans et al. 1983; Comans and Hockley 1992) and interstitial diffusion is considered negligible. The three principal sources of radiocesium to the coring site are inflow from Lake Superior, direct loading from the atmosphere to the river, and runoff from several watersheds. From the first two sources, significant numbers of  $^{137}\text{Cs}$  ions will be available to sequester with particles that are present at elevated concentrations in the river system. Capture of these ions must occur within short transit times as water passes through the St. Mary's River to Lake George. Along this pathway, initially pristine particles would encounter organic urban–industrial contaminants that may adhere to particle surfaces and compromise their adsorption capacity. Also biosolids from pulp and paper production, discharged into the river at Sault Saint Marie, may compete with mineral particles and weakly bind the radionuclide. Finally, weakly bound fractions of  $^{137}\text{Cs}$  may end up in an oil and grease rich sedimentary environment that is not conducive to adsorption on particles. In the 1986 core, concentrations of oils and greases between 1952 and 1986 averaged about 2500 ppm with concentrations as high as 8000 ppm in one core section (Upper Great Lakes Connecting Channels Study 1989). Such a process would apply to  $^{137}\text{Cs}$  only and would displace threshold locations downward without a major effect on peak positions and slowly broaden profiles, especially along trailing edges.

#### A history of sediment accumulation

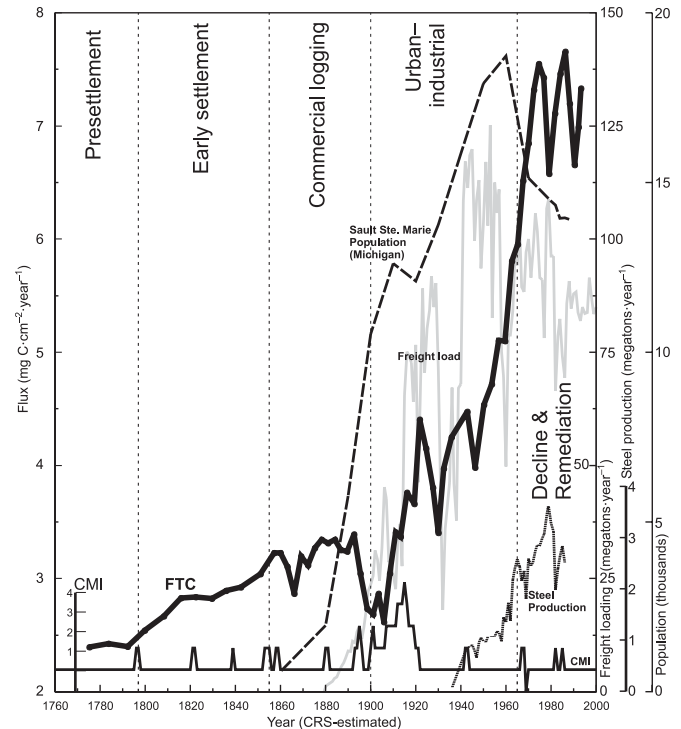
The CRS net rate of sediment accumulation (Fig. 3c, solid circles) is relatively constant ( $0.15 \text{ g}\cdot\text{cm}^{-2}\cdot\text{year}^{-1}$ ) from 1890

until the late 1940s and thereafter rises to a maximum ( $0.24 \text{ g}\cdot\text{cm}^{-2}\cdot\text{year}^{-1}$ ) in 1984. To assess the potential impacts of major physical alterations of the St. Mary's River on sedimentation rates in Lake George, we estimated the annual number of concurrent activities (between 1797 and 2000) involving construction, maintenance, or improvements (CMI) of locks, canals, power plants, and compensating works based on Kauss (1991) and supplemented by several additional sources (e.g., American Society of Mechanical Engineers 1981; Bayliss 2000; Northern Michigan University 2003). We included only those operations potentially contributing fine particles to Lake George. The resulting CMI index (Fig. 3c, shaded histogram, feature a) indicates that the largest number of concurrent operations took place from 1913 through 1916 and includes ongoing construction of the Compensating Works, construction of the Davis and Sabin locks, construction of the Canadian Canal, and expansion of the Canadian Great Lakes Power Corporation. A statistically significant increase in CRS sedimentation rate (about 20%) encompasses this period seen in the broad maximum (Fig. 3c, feature 1). Beyond 1940, there are only a few candidate events, the construction of the McArthur Lock from 1942 through 1943 (feature b) and the expansion of the Poe Lock from 1964 through 1968 (feature c). These are not associated with increases in sedimentation rate. There are also two maxima (features 2 and 3) in the sedimentation rate history for which there are no corresponding features in the CMI index. A pair of candidate events (feature d), the expansion of the Canadian Great Lakes Power Corporation (1981–1982) and construction of a berm in rapids near Whitefish Island (~1985), does coincide with a significant (~15%) increase in sedimentation rate (feature 4). This coincidence is consistent with observations of massive resuspension of red clay deposits from the river downstream of the Great Lakes Power Corporation following restart of operations in 1982 that more than doubled discharge capacity. This analysis indicates that developments and operations of the locks and associated structures at Sault Saint Marie had little impact on sedimentation rates in Lake George. The 60% increase in rates that commenced in the 1940s must be due to other causes.

### A history of TC accumulation

Apart from sharing a generally upward trend between 1890 and 1993, TC concentrations vary inversely with sediment accumulation rates (Fig. 3c). During periods when rates are minimal, about 20% lower on average with respect to a trend line, there is a complementary increase of about 20% in concentrations of TC and vice versa. Much of this complementarity is likely caused by dilution and can be removed by calculating a TC flux (FTC) to sediments (as TC in  $\text{mg}\cdot\text{g}^{-1}$  multiplied by  $r_s$  in  $\text{g}\cdot\text{cm}^{-2}\cdot\text{year}^{-1}$ ). It should be noted that TC itself is not a major diluent, since only  $8\% \pm 2\%$  of the sediment mass is associated with some form of carbon-containing matter, both organic matter, assumed to be represented by the semiempirical formula of  $\text{CH}_2\text{O}$ , and inorganic matter, assumed to be essentially all  $\text{CaCO}_3$ . On average, inorganic matter contributes  $22\% \pm 10\%$  of TC associated matter (inorganic matter plus organic matter), although the contributions in several core sections are about 50%. The trend of FTC with time is shown in Fig. 4 (thick

**Fig. 4.** Long-term history of carbon flux to Lake George sediments showing corresponding demographic and commercial data. The CMI index indicates the number of major construction, maintenance, or improvement activities occurring at sites in the St. Mary's River upstream of Lake George. CRS, constant rate of supply.



solid line) with major changes in nature and intensity of human impacts on the river and its watershed also illustrated (Fig. 4, vertical broken lines). The major increase starts around 1900 and follows rapid population growth and the subsequent increases in freight loading and steel production. The relative amount of TC in the sediments roughly followed metal concentrations (Fig. 5), but a more recent decline is not as obvious.

Over the 220-year period from about 1773 through 1993, FTC increased by a factor of 3. During the earliest period, presettlement (~1773–1790), FTC values were lowest and essentially constant ( $2.4 \text{ mg}\cdot\text{cm}^{-2}\cdot\text{year}^{-1}$ ). With the establishment of the first sawmill at Sault Saint Marie in 1783 (Fig 4, spike in CMI), FTC began to rise monotonically through the early settlement period (1790–1855), which was punctuated by a series of minor construction events in the river. During that period, only relatively small-scale farming and lumbering operations occurred in the region. During the initial phase (1855–1890) of the period of commercial logging, FTC continued to rise erratically. It then dropped considerably starting in 1895, a date that marks the beginning of a period of intense construction in the river. Reasons for the drop are unclear but could be due to suppression of organic matter production in the river system by construction activities or diminished organic matter loading from watersheds toward the end of the logging era. During the period of industrialization of the region (1900–1965), several features can be identified. The period of minimum FTC continued until about 1910. It then rose sharply during and after com-

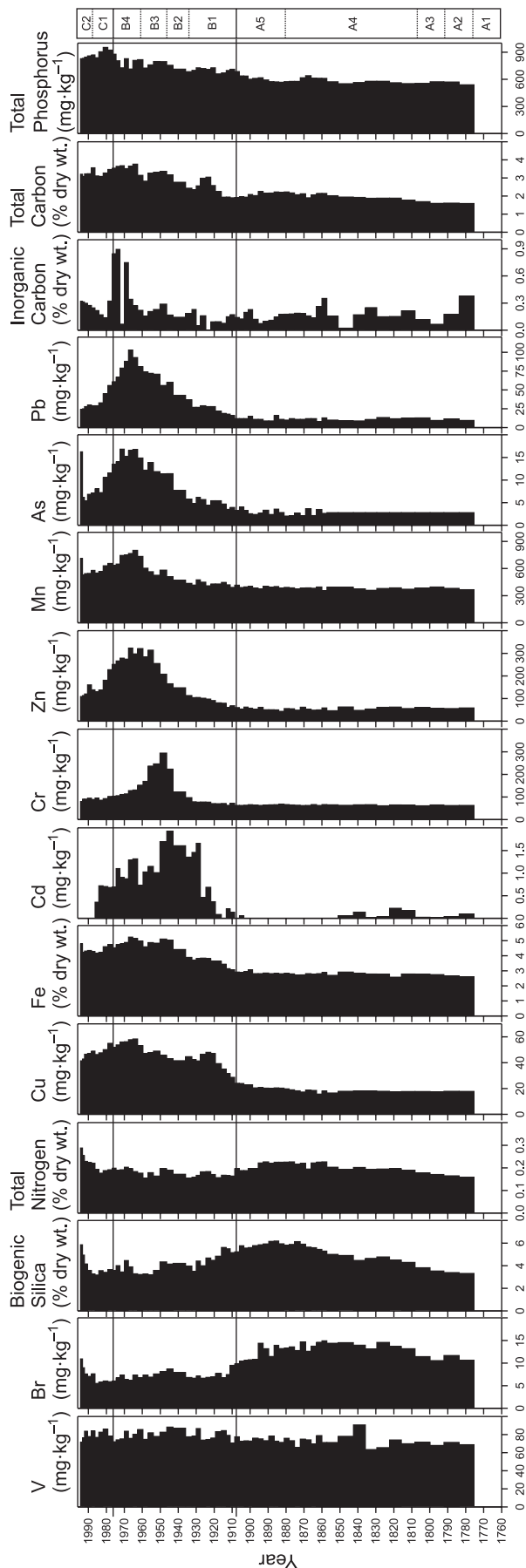


**Fig. 5.** Sediment chemical data from Lake George. Interval dates are shown on the left and zones, as determined by diatom-based cluster analysis, are presented on the right.

pletion of major construction projects and associated increase in loading of freight through the new locks. Around the 1930s, FTC declined and stalled through the depression era. The stall ended essentially with the onset of World War II. The steepest rise in FTC occurred during the war years, continued into the mid-1960s, and was associated with increased freight loading and steel production. Throughout the postconstruction part of the urban–industrial period (ca. 1920–1960), FTC tracked with the population of Sault Saint Marie. During the nearly 30-year period of industrial decline and environmental remediation (“decline and remediation”, from about 1965 to the core collection date, 1993), FTC has fluctuated around  $7.0 \pm 0.5 \text{ mg}\cdot\text{cm}^{-2}\cdot\text{year}^{-1}$ .

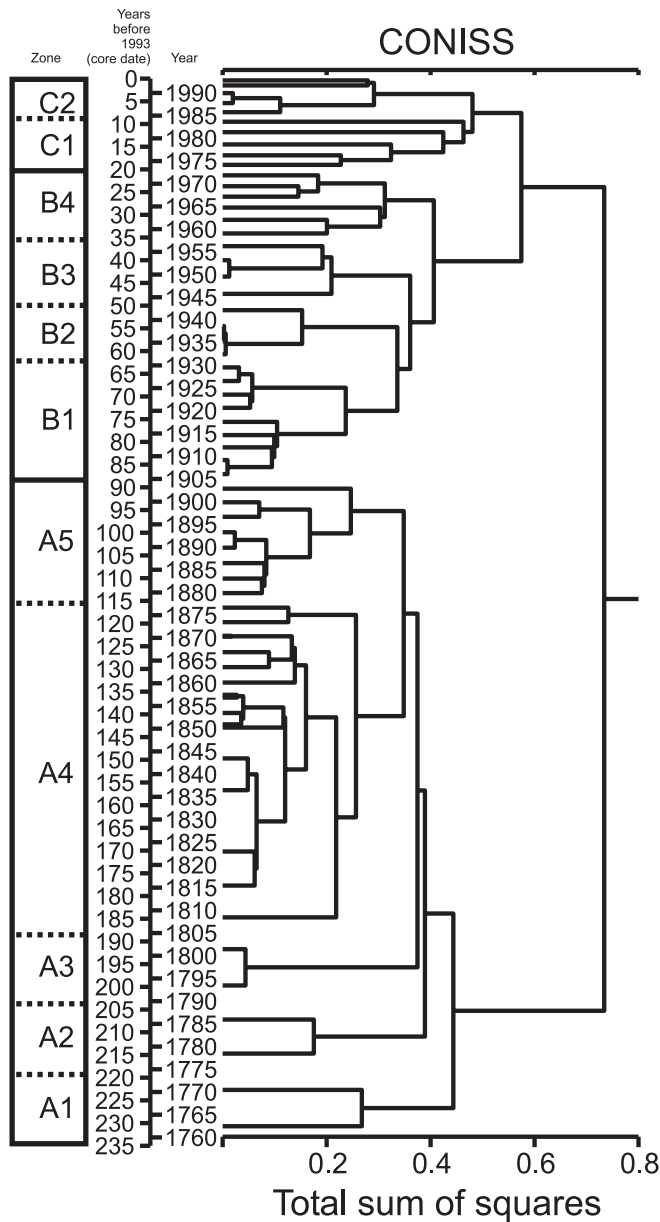
### Chemical trends

For 32 sedimentary compounds and elements (profiles of 15 shown in Fig. 5), factor analysis with varimax rotation distinguished four significant groups: two groups of mineral components, one marked by Ce, Eu, Sc, and Th (12% of variance) and the other by La, Lu, Sm, Ti, and Yb (10% of variance), that were largely invariant with respect to changes in sediment composition and core depth, particularly through the industrial period. These groups are not discussed further. The principal factor (accounting for 38% of variance) consisted of As, Cd, Co, Cr, Cu, Cs, Fe, Mn, Pb, Sb, Zn, TC, and TP plus four variables weakly associated with this group, Ca, Hf, V, and IOC. The strongly associated members of this group are mostly composed of well-known urban and industrial contaminants from iron and steel production (Fe, Mn, Co, and TC), production of alloys and metal coating processes (Cd, Co, Cr, Cu, Mn, Sb, and Zn), leather tanning (Cr and Cd), herbicides (As), lumber and pulp production (TC and TP), mining activities (Cu and Pb), and fuel additives (Pb). There is considerable redundancy in profiles within this group, with subtle differences that are not well resolved by statistical approaches. However, in general, representatives from this group started to increase at ~35 cm sediment depth, shortly after the beginning of the 20th century (Fig. 5, zone B; zonation by cluster analysis is presented in Fig. 6 and is discussed later), corresponding to growing mining, leather tanning, and other industries in the river catchment. Concentrations of Cd and Cr in the sediments continued to increase until ~1950. Since the late 1950s (when the Northwestern Leather Company closed), these metal concentrations have declined nearly to their preimpact levels. In the most recent sediments, Cd has declined to below instrumental detection limits. Although V is often linked to anthropogenic loading of metals, no notable increase in V from background concentrations occurred in the profile. Like TC, TP concentrations have increased gradually since 1900 from 500+ to over 900  $\text{mg}\cdot\text{kg}^{-1}$  in the late 1970s, suggesting an increasing anthropogenic nutrient load to the lake.

A fourth group (7% of variance) consisted of BSi, Br, TN, and two putatively mineral components, Al and Na. Biogenic Si, Br, and TN increase gradually throughout the 1800s



**Fig. 6.** Combined cluster analysis based on 62 common diatom species in sedimentary assemblages. Clustering was constrained by depth to construct zones (A, B, and C) and their subdivisions (separated by broken lines).



(zones A4 and A5), an early period in European settlement of the region. In the 1900s, BSi and Br concentrations decline (zones B and C1) but again increase within the uppermost decade represented in the core (Fig. 5). Bromine is known to be an essential element for some diatom species (Kerfoot et al. 1999), and Si comprises diatom cell walls, so these trends appear to reflect diatom populations in Lake George. Statistical relationships between sediment chemistry and diatom assemblages are discussed in a later section.

**General taxonomic trends**

A total of 448 diatom species in 47 genera were identified in the Lake George core. In addition, 77 (generally rare) types were similar to known taxa but could not be character-

ized according to species in the current literature, so they have been tentatively given a “cf.” identification. Prepared samples contained moderate amounts of clastic material, and 0.9% of diatom valves were too damaged or obstructed by clastics to be identified, and 1.0% of specimens could only be identified to the genus level. Common taxa are listed in Table 2, and a full list of diatoms identified in Lake George sediments is available from the authors.

A general observation of the relative abundance and accumulation rate profiles (Figs. 7 and 8) indicates that high relative abundance of a taxon does not necessarily reflect high productivity of that taxon. Although there were significant correlations between relative abundance and accumulation rates, particularly for dominant taxa (data not presented), there are cases where peaks of relative abundance do not represent higher productivity, such as for total planktonic taxa (Fig. 7), where a fairly smooth relative abundance profile is much more erratic when presented as accumulation rates. We recommend caution when assuming direct correlations between relative abundance and productivity for diatoms in fluvial systems like Lake George.

The hierarchical tree for the cluster analysis (Fig. 6) indicates the extent of similarity between diatom assemblages at different intervals in the core. The highest order of differentiation (sum of squares) distinguishes samples deposited before ~1904 from those deposited since then. This major distinction allowed the definition of zone A, the early period, and a recent period. The recent zone could be subdivided into B (~1904–1973) and C (~1973–1993). The broken-stick model testing (Bennett 1996, 2002) indicated that these three zones accounted for interpretable proportions of the variance in the diatom data. Based on cluster analysis, further subdivisions (broken lines in Fig. 6) were derived within these three zones, but these subzones did not account for significant amounts of variation. We maintained these subdivisions to provide general information on the more subtle transitions in the diatom assemblages and to aid in stratigraphic interpretation. The zonation and its relationship to the history of the region are discussed in more detail in the context of temporal shifts in the diatom assemblages.

The majority of the fossil diatom assemblages were composed of benthic diatoms, ranging from 48% to 89% of the total assemblage (Fig. 7). A distinct shift in relative abundance occurs around the turn of the 20th century as planktonic taxa increased, peaking at 55% in ~1945. For many genera, shifts in diatom relative abundance over the last two centuries were subtle, but some increases in planktonic genera (e.g., *Aulacoseira*, *Cyclotella*, and *Tabellaria*) clearly occurred in zones B and C. Profiles of the individual species (Figs. 7 and 8) track diverse assemblage trends.

Ratios of chrysophyte stomatocysts and scales to diatoms indicate an increase in scales relative to diatom frustules during the 20th century, with a peak in the 1950s, and accumulation rates of chrysophyte remains increased in zones A5 and B (Fig. 7). Accumulation rates reflect fluctuations throughout the microfossil profile, but overall trends indicate that accumulation rates of fossil chrysophyte remains more recent than ~1850 averaged higher than those observed in the bottom of the core. The increase in chrysophyte scales relative to diatom frustules reflects a more productive planktonic community throughout zone B, corresponding to the

**Table 2.** Common diatom taxa identified in the Lake George sediment cores.

Species	Code	No. of occurrences	Maximum relative abundance (%)
<i>Achnanthes minutissima</i> var. <i>scotica</i> (Carter) Lange-Bertalot	ACMINUVS	33	2.2
<i>Achnanthes oestrupii</i> (Cleve-Euler) Hustedt	ACOESTRU	18	2.2
<i>Achnantheidium minutissimum</i> (Kützing) Czarnecki	ACMINUTI	64	18.5
<i>Amphora inariensis</i> Krammer	AMINARIE	49	2.3
<i>Amphora pediculus</i> (Kützing) Grunow ex A. Schmidt	AMPEDICU	60	5.6
<i>Asterionella formosa</i> (Kützing) Grunow ex A. Schmidt	ASFORMOS	53	5.1
<i>Aulacoseira alpigena</i> (Grunow) Krammer	AUALPIGE	36	4.3
<i>Aulacoseira</i> cf. <i>islandica</i> (O. Müller) Simonsen	AUCFISLA	38	4.0
<i>Brachysira vitrea</i> (Grunow) Ross	BRVITREA	57	3.8
<i>Cocconeis neothumensis</i> Krammer	CONEOTHU	49	3.0
<i>Cocconeis placentula</i> var. <i>euglypta</i> (Ehrenberg) Grunow	COPLACVE	50	2.6
<i>Cyclotella bodanica</i> var. <i>lemanica</i> (O. Müller) Bachmann	CYBODAVL	50	3.9
<i>Cyclotella</i> cf. <i>comensis</i> Grunow	CYCFCOME	4	6.8
<i>Cyclotella</i> cf. <i>distinguenda</i> Hustedt (small)	CYCFDIST	4	2.6
<i>Cyclotella comensis</i> Grunow	CYCOMENS	19	13.4
<i>Cyclotella comta</i> var. <i>unipunctata</i> Hustedt	CYCOMTVU	42	5.8
<i>Cyclotella michiganiana</i> Skvortzow	CYMICHIG	45	2.9
<i>Cyclotella ocellata</i> Pantocsek	CYOCCELLA	64	11.1
<i>Cyclotella radiosa</i> (Grunow) Lemmermann	CYRADIUS	30	3.2
<i>Cyclotella stelligera</i> Cleve and Grunow	CYSTELLI	49	3.2
<i>Cyclotella stelligeroides</i> Hustedt	CYPSEOID	64	20.1
<i>Cymbella delicatula</i> Kützing	CMDELICA	57	4.1
<i>Denticula keutzingii</i> Grunow	DEKEUTZI	49	3.0
<i>Diatoma tenuis</i> Agardh	DIATENUI	15	2.3
<i>Encyonema silesiacum</i> (Bleisch) D. G. Mann	ENCSILES	49	4.5
<i>Encyonopsis cesatii</i> (Rabenhorst) Krammer	ENOPCESA	36	2.3
<i>Encyonopsis krammeri</i> Reichardt	ENOPKRAM	22	2.3
<i>Encyonopsis subminuta</i> Krammer and Reichardt	ENOPSUBM	47	3.5
<i>Eucocconeis flexella</i> (Kützing) Cleve	EUFLEXEL	61	4.6
<i>Fragilaria capucina</i> Desmazières	FRCAPUCI	14	2.0
<i>Fragilaria capucina</i> var. <i>gracilis</i> (Østrup) Hustedt	FRCAPUVG	27	2.9
<i>Fragilaria capucina</i> var. <i>mesolepta</i> (Østrup) Hustedt	FRCAPUVM	3	12.5
<i>Fragilaria capucina</i> var. <i>vaucheriae</i> (Kützing) Lange-Bertalot sensu lato	FRCAPUVV	62	27.2
<i>Fragilaria crotonensis</i> Kitton	FRCROTON	61	9.7
<i>Fragilaria nanana</i> Lange-Bertalot	FRNANANA	21	2.2
<i>Fragilaria robusta</i> (Fusey) Manguin	FRROBUST	9	3.2
<i>Gomphonema pumilum</i> (Grunow) Reichardt & Lange-Bertalot	GOPUMILU	56	3.6
<i>Karayevia clevei</i> (Grunow) Bukhtiyarova & Round	KACLEVEI	36	2.2
<i>Navicula</i> cf. <i>kuelbsii</i> Lange-Bertalot	NACFKUEL	2	3.7
<i>Navicula cryptotenella</i> Lange-Bertalot	NACRELLA	57	3.2
<i>Navicula cryptotenelloides</i> Lange-Bertalot	NACRYOID	45	2.3
<i>Navicula submuralis</i> Hustedt	NASUBMUR	59	5.3
<i>Nitzschia angustata</i> Grunow	NIANGUST	26	2.1
<i>Nitzschia dissipata</i> var. <i>media</i> (Hantzsch) Grunow	NIDISSVM	14	2.6
<i>Nitzschia frustulum</i> (Kützing) Grunow	NIFRUSTU	25	2.2
<i>Nitzschia gracilis</i> Hantzsch	NIGRACIL	21	2.2
<i>Nitzschia paleacea</i> (Grunow) Grunow	NIPALEAC	20	2.5
<i>Nitzschia perminuta</i> (Grunow) M. Peragallo	NIPERMIN	7	2.6
<i>Planothidium lanceolatum</i> (Brébisson) Bukhtiyarova & Round	PLLANCEO	27	3.7
<i>Psammothidium abundans</i> f. <i>rosenstockii</i> (Lange-Bertalot) Bukhtiyarova	PSABUNVR	48	2.9
<i>Pseudostaurosira brevistriata</i> (Grunow) D.M. Williams & Round	PTBREVIS	55	7.7
<i>Pseudostaurosira</i> sp. 1 (possibly <i>P. brevistriata</i> var. <i>inflata</i> (Pantocsek) M.B. Edlund)	FRSPI	53	6.3
<i>Rossethidium pusillum</i> (Grunow) Bukhtiyarova & Round	ROPUSILLA	7	2.3
<i>Staurosira construens</i> Ehrenberg	SACONSTR	56	10.4

**Table 2** (concluded).

Species	Code	No. of occurrences	Maximum relative abundance (%)
<i>Staurosira construens</i> var. <i>binodis</i> (Ehrenberg) Hamilton	SACONSVB	10	5.8
<i>Staurosira construens</i> var. <i>venter</i> (Ehrenberg) Hamilton	SACONSVV	30	7.0
<i>Staurosirella leptostauron</i> (Ehrenberg) D.M. Williams & Round	SAELEPTO	30	2.7
<i>Staurosirella pinnata</i> (Ehrenberg) D.M. Williams & Round	SAEPINNA	64	15.9
<i>Staurosirella pinnata</i> var. <i>acuminatum</i> (A. Mayer) D.M. Williams & Round	SAEPINVA	44	2.9
<i>Staurosirella pinnata</i> var. <i>lancettula</i> (Schumann) Poulin	SAEPINVL	29	3.1
<i>Tabellaria flocculosa</i> (Roth) Kützing str. 3P sensu Koppen	TAFLOC3P	64	6.3
<i>Tabellaria quadriseptata</i> Knudson	TAQUADRI	55	3.1

**Note:** Species were identified as common if they occurred in at least two samples with at least 2% abundance in one or more samples.

increased local human population and associated nutrient load during this period (Figs. 4 and 5).

### Planktonic taxa

The abundance of the genus *Cyclotella* was highest in zone B, but individually, the profiles of *Cyclotella* taxa varied. The small taxon *Cyclotella* cf. *comta* var. *unipunctata* was most abundant during the onset of intense settlement (Fig. 8, upper zone A). Several taxa (including *Cyclotella bodanica* var. *lemanica*, *Cyclotella ocellata*, and *Cyclotella stelligeroides*) were most abundant throughout zone B, but relative abundance decreased in zone B2 (Figs. 7 and 8). The most recent sediments of zone C (C2, approximately the uppermost 5 years) contained high numbers of *Cyclotella comensis* valves. These trends in *Cyclotella* species correspond to the overall increase in planktonic taxa in postsettlement sediments. Individually, these taxa do not necessarily indicate nutrient enrichment, but the shift to an increasingly planktonic assemblage indicates greater planktonic productivity. The recent peak of *Cyclotella comensis* was also observed in Lake Erie (Stoermer et al. 1996), corresponding to the recent period of epilimnetic nutrient declines, and so its appearance in the most recent few years may reflect lower nutrients than in the 1970s and 1980s.

In our core samples, *Aulacoseira alpigena* fluctuated in abundance throughout zones A and B; however, *Aulacoseira* cf. *islandica* was relatively rare in earlier sediments and achieved its highest relative and absolute abundance in zones B and C. Although we are uncertain if *Aulacoseira* cf. *islandica* is the nominate form of *Aulacoseira islandica*, this taxon is a synonym of *Melosira islandica*, which has been observed in the sediments of Lakes Superior, Michigan, and Ontario (Stoermer and Ladewski 1976; Thayer et al. 1983a; Stoermer et al. 1985a). In contrast with previous studies from Lakes Michigan and Ontario, *Aulacoseira* cf. *islandica* is mainly a postsettlement taxon, reflecting the increase in plankton that occurred in the system after early human development in the region. Thayer et al. (1983a, 1983b) noted a high relative abundance of *Melosira islandica* in the recent sediments of cores from Lake Superior, upstream of Lake George. As in other areas of the Great Lakes, we ascribe the higher abundances of *Aulacoseira* cf. *islandica* between ~1903 and 1968 to moderate nutrient enrichment.

Planktonic species of *Fragilaria* were also favoured following human settlement of the watershed. *Fragilaria capucina* var. *vaucheriae* and *Fragilaria crotonensis* peaked in

the most recent sediments (zones B3 through C2), indicating a productive planktonic assemblage in recent decades. *Fragilaria crotonensis*, in particular, is a common indicator of higher nutrient levels in the Great Lakes (Hartig 1987). Other planktonic taxa include the high-nutrient *Diatoma tenuis*, which obtained a marked high abundance in zone C.

### Benthic taxa

Benthic and tychoplanktonic species of fragilarioid taxa dominated between ~1850 and 1900 (Figs. 7 and 8), with particular reference to *Pseudostaurosira brevistriata*, *Staurosira construens*, *Staurosirella pinnata*, and an unidentified taxon (*Pseudostaurosira* sp. 1), which has similarities to *Pseudostaurosira brevistriata* var. *inflata*. These taxa tend to be cosmopolitan and are often noted in both plankton and benthic assemblages (Stoermer 1980). A similar trend for *Staurosira construens* and *Staurosirella pinnata* has been observed in Lake Ontario (Stoermer et al. 1985a). This trend may reflect a temporary increase in epilithic and epipsammic taxa in response to watershed clearance and outwash of clastic material to the Great Lakes. Construction of locks and canals, combined with continued clearcutting of forests in up-gradient watersheds, makes this a likely scenario for the observed trends in these small fragilarioid taxa. Other species (e.g., *Staurosira construens* var. *binodis* and *Staurosira construens* var. *venter*) appeared sporadically throughout the past 230 years.

Raphid diatom taxa had complex relative abundance profiles in the Lake George core, but a few overall trends are apparent in the accumulation rates of epiphytic taxa. *Eucocconeis flexella*, *Achnantheidium minutissimum*, and *Cymbella delicatula* peaked in the upper portion of zone A (A5) followed by low accumulation rates through zone B. The accumulation rates of epiphyton recovered in zone C. This gross trend parallels the trend for the benthic totals (Fig. 7) and indicates the notable transitions in diatom assemblages that have occurred during the recent history of Lake George.

Finally, although each taxon occurred in low relative abundance, *Nitzschia* peaked during varying periods in the system's recent history. *Nitzschia angustata*, *Nitzschia dissipata* var. *media*, and *Nitzschia perminuta* peaked in the upper section of zone A. *Nitzschia frustulum* and *Nitzschia palaeae* peaked in zone C. Grouped by genus, *Nitzschia* is present in highest proportions in zone C and tends to be less abundant in deeper intervals (Fig. 7).



**Fig. 7.** Sedimentary profiles of diatom groups, chrysophyte/diatom ratios, and common diatoms (greater than 10% abundance in any sample). (a) Relative abundance and (b) absolute accumulation rates are provided for the diatom sum, ratios of chrysophyte scales and cysts to diatoms, planktonic taxa, araphid taxa, monoraphid taxa, *Navicula*, and *Nitzschia*. Interval dates are shown on the left and zones, as determined by diatom-based cluster analysis, are presented on the right.

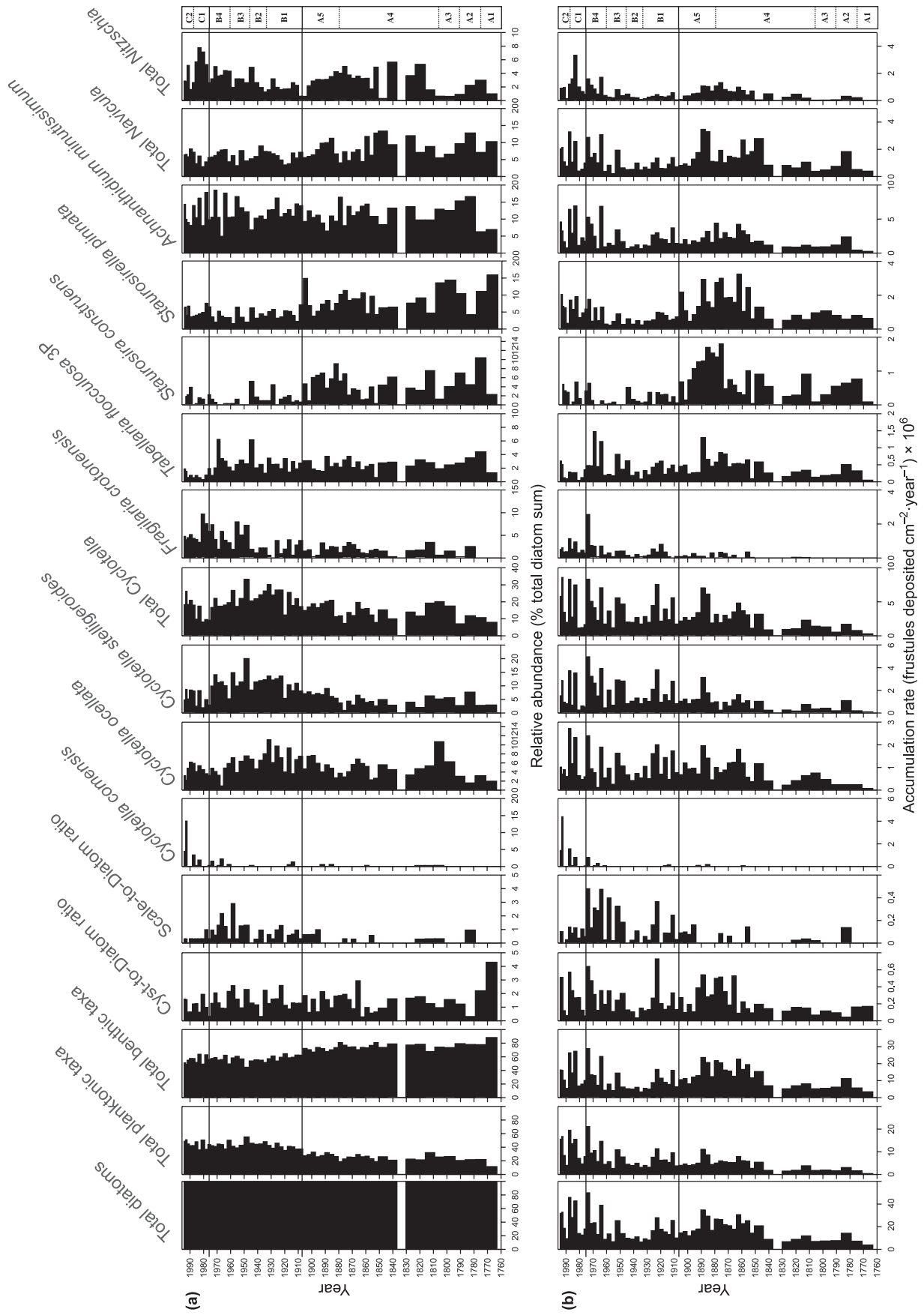


**Fig. 8.** Sedimentary profiles of diatom species with relative abundances between 5% and 10% in any sample from the Lake George sediment cores. Some less abundant species were included because of notable trends and important indicator properties. Profiles represent (a) relative abundance and (b) absolute accumulation rates. Interval dates are shown on the left and zones, as determined by diatom-based cluster analysis, are presented on the right.

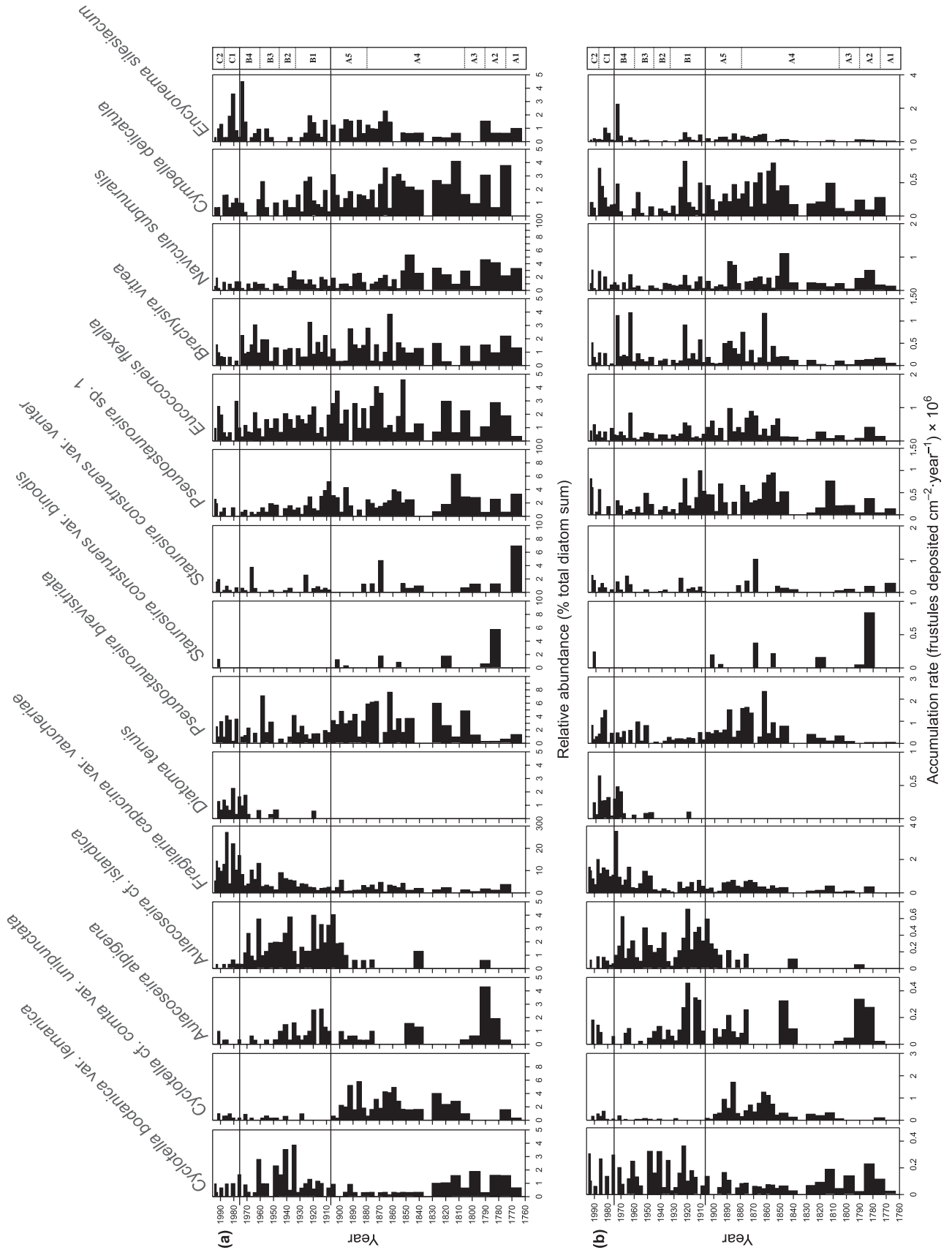


**Fig. 9.** CCA of diatom assemblages and sediment chemistry. (a) Sample ordination relative to the nine forward-selected chemical variables; (b) species scores relative to these variables. Axes are in standard deviation units. Species codes correspond to the codes in Table 2.

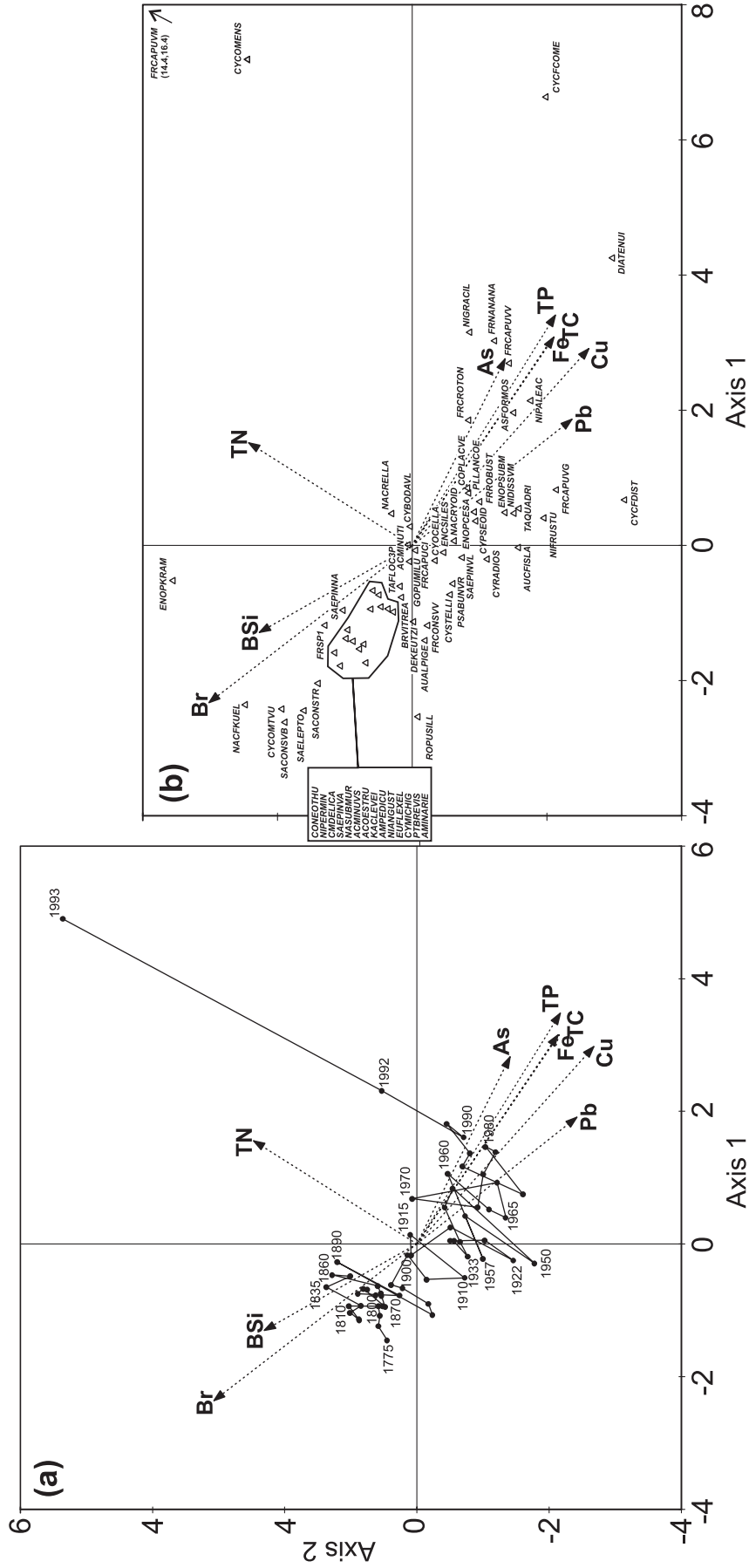
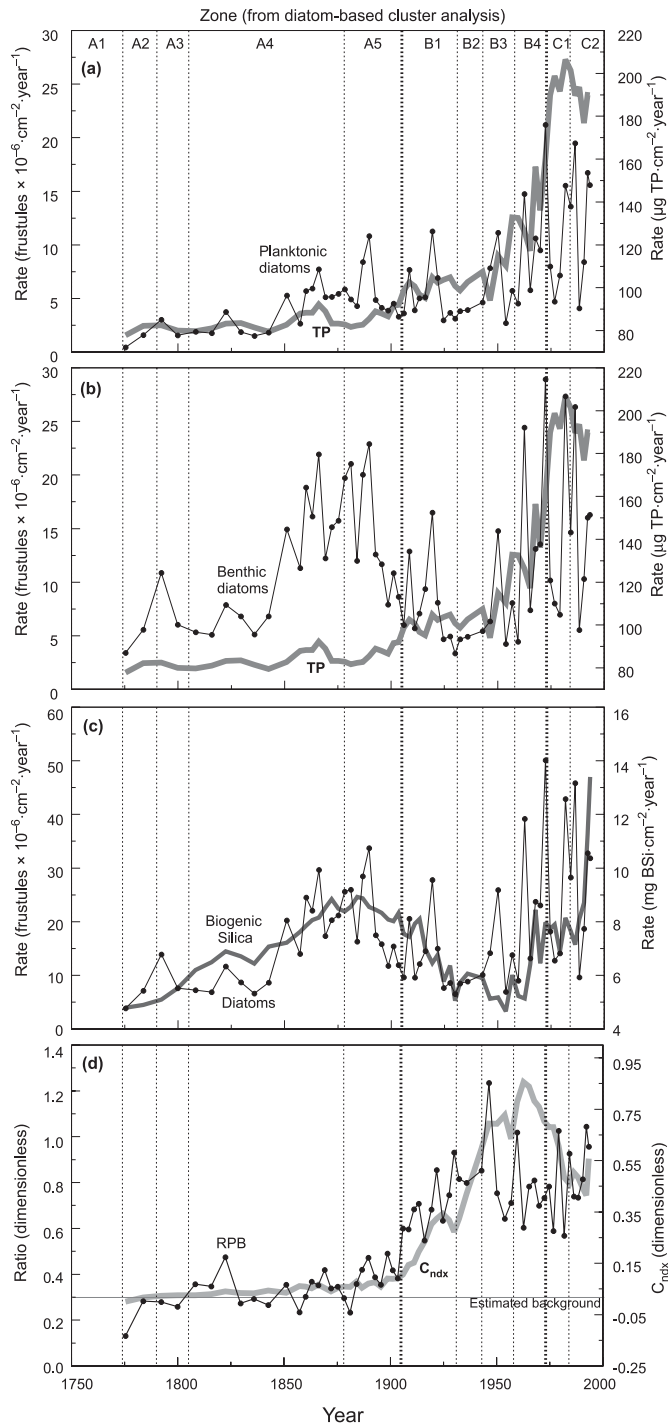




**Fig. 10.** Relationships between diatoms and selected chemical trends in the sedimentary profile from Lake George. (a) Planktonic diatom and total phosphorus (TP) accumulation rates; (b) benthic diatom and phosphorus accumulation rates; (c) diatom and BSi accumulation rates; (d) ratio of planktonic to benthic diatoms compared with the contamination index ( $C_{ndx}$ ).



**Diatom–chemical relationships**

During CCA, out of the 32 sedimentary environmental variables, forward selection identified nine variables that could effectively explain the maximum amount of variance

in the diatom data (Fig. 9). This subset of variables included, in order of selection, TP, TN, As, Pb, BSi, Fe, TC, Cu, and Br (Monte Carlo, 999 permutations,  $P < 0.05$ ). The remaining 23 variables had no significant correlation with patterns in the diatom assemblages or are redundant (i.e., they do not independently capture variation in the diatom data). This large number of redundant variables is not surprising given the number of metals that have similar trends in the paleolimnological profile (Fig. 5) and so would be highly inter-correlated. Based on the placement of variables on the ordination plot (Fig. 9), much correlation among variables remains. For example, although the axes 1 and 2 scores for Fe and TC almost lie on top of each other, enough independent variation in the diatom data could be explained by each of these variables to allow them both to be chosen during forward selection.

The eigenvalues for CCA axes 1–4 (0.14, 0.11, 0.06, and 0.04) constrained to these nine environmental variables were all significant ( $P < 0.05$ ), and species–environment correlations (axis 1 = 95.2%, axis 2 = 91.2%, axis 3 = 85.9%, and axis 4 = 80.7%) were high, suggesting that the subset of nine variables could account for a large proportion of the variance explained within the data. Based on the eigenvalues of the first four axes, axes 1 and 2 merit more detailed interpretation.

Based on canonical coefficients of the environmental variables (ter Braak 1995; ter Braak and Šmilauer 2002), CCA axes 1 and 2 captured a strong pollution gradient ranging from clean, presettlement conditions in the upper left quadrant to polluted 20th century conditions in the lower right quadrant (Fig. 9). To conclude that metals variables such as As, Fe, and Pb have had a direct influence on diatom communities in Lake George would be premature. It is more likely that these variables serve as proxies for intercorrelated groups of metals and for a more general pollution index (see  $C_{ndx}$  discussion below). A number of studies have shown the influence of TP on diatom distribution in North America (e.g., Reavie et al. 1995; Dixit et al. 1999), and it is likely that this variable has had a more direct influence on the diatom communities in the lake.

The ordination diagram on the left illustrates the trajectory of samples over time relative to environmental variables (Fig. 9; Table 2). As can be confirmed by observing trends in the chemical profiles (Fig. 5), the 1800s was a time of relatively high accumulation of Br and BSi, whereas the 1900s exhibited relatively high metal and nutrient concentrations. The major excursion of the trajectory into the upper right quadrant reflects significant increases in concentration toward the sediment surface of two groups of elements that exhibited contrary behaviour elsewhere in the core. Concentrations of BSi, Br, and TN increase gradually from about 3–4 cm to the surface with ratios  $C_{0-1}/C_{3-4}$  of 1.68, 1.55, and 1.28, respectively. Concentrations of another four elements, As, Mn, Ca, and Fe, increase abruptly from 1–2 to 0–1 cm. The ratios  $C_{0-1}/C_{1-2}$  are 2.62, 1.35, 1.29, and 1.14, respectively. For all other elements, values of  $C_{0-1}/C_{1-2}$  average  $0.99 \pm 0.04$  with a range 0.91–1.05. We believe that surface enrichment of the first three elements is due to an initial, relatively high rate of dissolution of BSi and associated elements (Br and TN) that decreases rapidly as deposited frustules are buried and encounter a Si-saturated pore

water environment. Elevated surface concentrations of As, Mn, and Fe but not Ca could be due to chemical diagenesis where small amounts of redox-sensitive elements (As, Mn, and Fe) may dissolve in anoxic sediments, diffuse through pore water, and precipitate in oxic surface sediments. Alternatively, elevated surface concentrations of the four elements could in principle reflect recent increases in anthropogenic loading or be due to near-surface particle sorting that may elevate concentrations of fine particles at the interface. However, the hypothesis of anthropogenic loading seems to be inconsistent with the recent history of potential sources (principally iron and steel production), while interfacial particle sorting should affect many elements that are not surface enriched.

The ordination diagram on the right clearly illustrates the corresponding shift in diatom assemblages over time in response to ecosystem modifications. Several diatom taxa (e.g., *Staurosira construens*, *Staurosirella pinnata*, *Cocconeis neothumensis*, and *Cymbella delicatula*) are clustered in the pre-1900 region of the plot, indicating that these taxa characterized the assemblage prior to the onset of significant anthropogenic disturbance. More pollution-tolerant taxa (e.g., *Asterionella formosa*, *Fragilaria crotonensis*, and *Diatoma tenuis*) correspond to 20th century samples, at the high end of the pollution gradient. A number of taxa, including *Achnanthydium minutissimum* and *Gomphonema pumilum*, occur near the origin because their relative abundance showed no trend over time related to environmental shifts, and they are probably tolerant of a wide range of environmental conditions.

In summary, CCA ordination suggests that there are statistically significant relationships between diatom distributions and a 300-year shift in the pollution gradient for Lake George based on correlations with sedimentary chemical indicators. Also, a number of these diatom taxa specifically reflect presettlement, postsettlement, and cosmopolitan assemblages, which can in the future be used to identify disturbance in sediment cores from the Great Lakes.

The relationships between diatom accumulation and sediment chemistry, including fluxes for diatoms, TP, and BSi, show that there is a broad increase in benthic diatom flux during the period of commercial logging operations and little response from planktonic taxa (Figs. 10a and 10b, upper zone A4 and zone A5). This period was prior to the large anthropogenic nutrient loading, which started in zone B. A similar situation was encountered in Lake Erie by Schelske et al. (1983). Schelske et al. (1983) noted an increase in BSi peaking around 1900 that was associated with forest clearance, while significant increases in TP occurred much later (the 1960s) when notable eutrophication occurred. In Lake George, during the early period of high benthic diatom flux (ca. 1850–1900), there were only small, uncorrelated changes in FTP, while the total diatom flux tracked closely with BSi flux (Fig. 10c). From these trends, we conclude that (i) Si was mobilized within watersheds during the commercial logging period and converted to diatom mass en route to or within Lake George, (ii) utilization of Si (BSi production) required relatively small levels of nutrients in the naturally oligotrophic lake, and (iii) only a small increase in TP flux was associated with increased benthic diatom flux before 1900. Not surprisingly, diatom flux increases,

albeit erratically, through zone B with the increase in anthropogenic nutrient loading. The decline in diatom abundance, even temporary disappearance of some taxa (Figs. 7 and 8, accumulation rate panels) and the associated minimum BSi between about 1930 and 1955 (primarily zone B3), is associated with the period of highest metal concentrations (especially Cr, Cd, and Cu) among the contaminant elements reported in this study, reflecting the probable impact of metals contamination on diatom productivity.

The ratio of planktonic diatom flux to benthic diatom flux (RPB) is relatively constant in zones A1–A3 and most of A4. The ratio begins to increase significantly from 1850 (end of zone A4) into zones A5 and B (Fig. 10d), a trend that parallels the contamination index  $C_{ndx}$ . The major shift in RPB begins at the turn of the 20th century as the system became impacted by contaminants, but it is clear that the composition of diatom fossil records cannot be explained solely by nutrient availability. From zone B3 through zone C,  $C_{ndx}$  continues to rise and then declines, whereas RPB shows no apparent trend. This dichotomy in trends for RPB and  $C_{ndx}$  may be a result of a lower Si supply from watersheds following the decline in forest clearance and logging operations. The occurrence of lightly silicified diatom taxa such as *Asterionella formosa* during this period supports this conclusion; however, long-term data from the Lake Superior outflow indicate no decline in Si concentration (Schelske 1984), so reasons for this shift remain uncertain.

## General discussion

Despite being a fluvial ecosystem, the anthropogenic environmental impacts that have occurred in Lake George can be tracked using paleolimnological methods. The cores allow the study of geochronological changes in response to contamination and other impacts related to human development. Some of our long-term observations are similar to trends observed in adjacent Great Lakes, including Lakes Superior (Stoermer et al. 1985b), Michigan (Stoermer et al. 1990), and Huron (Wolin et al. 1988). However, several observations are unique to Lake George as a result of its distinct environmental stress as well as the accumulation of local riverine diatoms.

The sedimentary record from the two Lake George cores can be divided into three environmental zones. Zone A starts in the 1700s when the system was unperturbed and captures preindustrial activities and environmental impacts as they increased toward 1900. Zone B is an interval from ~1905 to ~1970 in which urban–industrial and other cultural activities increasingly affected the structure of the diatom community. Zone C is an interval from ~1970 to ~1993 when rapid changes in the planktonic assemblage occurred, reflecting abatement of contaminant inputs.

One of the main stratigraphic events observed in our profile is the gradual relative increase in planktonic diatom taxa that starts in the late nineteenth century. Although similar studies do not exist for lotic ecosystems, models of nutrient enrichment in shallow lakes show that macrophytes typically dominate when nutrient loading is low, whereas phytoplankton dominate when nutrient loading increases above a critical threshold (Scheffer et al. 1993; Moss et al. 1996). A similar situation is probably true for Lake George. Despite having a high flushing rate, Lake George has maintained a relatively high abundance of plank-

tonic diatoms, in contrast with other fluvial sediments that are dominated by epilithic and epiphytic taxa (e.g., the St. Lawrence River; Reavie et al. 1998).

As observed in a paleoecological study of a fluvial lake in the St. Lawrence River (Reavie et al. 1998), the response of the plankton communities to human development was gradual throughout the late 19th and 20th centuries. The point of greatest transition in Lake George's history is not well defined, but the general trend is similar to trends observed from cores taken from other areas of the Great Lakes – St. Lawrence system. In Lake Ontario, for example, a gradual increase in planktonic taxa occurred between 1900 and 1945, apparently as a result of anthropogenic modification of nutrient loadings to the lake (Stoermer et al. 1985a; Schelske 1991). Locally, there have been numerous activities that would have increased nutrient loading and favoured planktonic assemblages in Lake George. The most intense period of agricultural development occurred in the Sault Saint Marie region during the transition to the 20th century (zone A5), and hydropower structures were built in 1898 just upstream of Lake George, resulting in controlled flow and an increase in lake recharge time. By increasing nutrient loads and slowing the flow of water through the lake, planktonic assemblages were apparently favoured, and the relative abundance of benthic taxa was depressed.

In the late 19th century (upper zone A4 and zone A5), the local population was growing, forest clearance and log booming peaked, and development of agriculture in the watershed was increasing rapidly. Furthermore, this period marked a major hydrologic change, with the construction of shipping locks and channels. The ecological changes resulting from these activities are reflected in the diatom record; a distinct assemblage change at ~1900 (distinguishing zones A and B). Throughout the 20th century until ~1970, industry continued to develop rapidly. Major sources of contamination to the lake have undoubtedly been the Algoma steel mill and St. Mary's Paper in Sault Saint Marie. Hesselberg and Hamdy (1987) noted in an analysis of several short sediment cores from the St. Mary's River that peak concentrations of contaminants (polychlorinated biphenyls, polycyclic aromatic hydrocarbons, and others) occurred in Lake George in the 1960s. This contamination had started to decline rapidly in the 1970s, marking the time of the diatom species inferred transition from zone B to zone C.

Zone B also marks the period of higher deposition of metals in the sediments. The increase in metals is largely attributed to pollution from a now defunct tannery (the Northwestern Leather Company), which was located upstream of the Sault Saint Marie Locks. Although the tannery went out of business in the late 1950s, a dumpsite of metallic debris remained long afterward. Soil and sediment samples from the dumpsite showed that the site was heavily contaminated with Cr, Cu, and Pb (Kenaga 1979), thus explaining why metals continued to be deposited downstream in Lake George, long after tanning activities ceased. Cadmium, which is often used in yellow pigments in the tanning process, was only measured at trace levels at the dumping site. Cadmium may have once existed at this site at higher concentrations, but it is likely that high Cd concentrations in the most recent sediment core came from metal-coating processes at the steel mill.

Zone C comprises sediments deposited after the US–Canada Great Lakes Water Quality Agreement of 1972, which has generally improved water quality in the Great Lakes (International Joint Commission 1997). However, based on the diatom profiles, a concomitant improvement cannot be confirmed for Lake George. This zone is characterized by high-nutrient planktonic taxa such as *Diatoma tenuis* (Van Dam et al. 1994), *Fragilaria crotonensis*, and varieties of *Fragilaria capucina*. However, during the most recent ~5 years represented in the core, the peak in *Cyclotella comensis* probably reflects the recent changes that may have resulted from water quality improvements. However, despite the lower overall phytoplanktonic standing crop in the Great Lakes, no concurrent decrease has yet been observed in the St. Mary's River. More than a decade has passed since the most recent core was taken from Lake George, and a followup investigation would be valuable to determine the impact of recent modifications to the fluvial ecosystem.

Now that an investigation of past diatom communities has been performed for Lake George, we argue that a previous speculation that algal productivity decreased after 1900 (Tenzer et al. 1999) is not strictly correct. J.A. Robbins (unpublished data) noted a decline in sedimentary BSi since 1900, suggesting a possible decline in diatom populations. However, while there was an evident reduction in diatom frustule mass flux to the sediments during the middle of the 20th century, frustule deposition in zones B4 and C is the highest yet for the last two centuries. It is possible that as nutrient inputs increased and the transition to a plankton-dominated system occurred, the available Si was being readily used by more lightly silicified planktonic diatoms such as *Nitzschia*, which increased in absolute and relative abundance in the recent sediments.

Lake George receives most of its water directly from Lake Superior, just upstream. While it would be expected that Lake George's diatom profile would be similar to that of Lake Superior, this generally is not the case. The diatom assemblages retrieved from Lake George sediments exhibited a high diversity owing to a variety of planktonic and benthic source habitats. Diatom frustules accumulating in Lake George are likely coming from the river itself, adjacent tributaries, littoral periphytic communities, and upstream planktonic communities. It is also likely that some of the sedimentary diatoms have been resuspended from Lake Superior and deposited. However, based on an assessment of common diatom species from Lake Superior (Thayer et al. 1983a, 1983b), we infer that contributions from Lake Superior have been minimal. Thayer et al. (1983a) performed a paleolimnological investigation of diatom remains from four Lake Superior sediment cores. They reported finding some of the same taxa, including *Asterionella formosa* and *Aulacoseira islandica*. However, the most common sedimentary diatom from the Lake Superior cores was the planktonic *Stephanodiscus transilvanicus*, while in Lake George, this taxon was encountered only once in an interval from approximately the 1860s. Although the genus *Stephanodiscus* has been an important indicator in paleolimnological investigations of nutrient trends in the Great Lakes (e.g., Stoermer et al. 1985b, 1989), the genus generally made up a small proportion of the assemblage in Lake George. We conclude, then, that the Lake George basin has not been capturing large



amounts of plankton transported from Lake Superior but accumulated sediments from the river upstream of Lake George and watersheds with tributaries to the river and upper portion of Lake George.

Although paleolimnological studies of fluvial lakes like Lake George can be challenging because of potential irregularities in deposition rates, sediment compositional stratigraphy, and mixing, such problems can be overcome with thorough cross-validation of stratigraphic markers. In this study, we have shown that codetermination of contaminant and nutrient signatures with siliceous microfossil profiles provides a powerful means of reconstructing ecological effects of human disturbances of the natural environment.

## Acknowledgments

We gratefully acknowledge the help of Y. Yamdy and P. Kauss, Ontario Ministry of the Environment, for their help in acquisition of the sediment core collected in 1986. We are indebted to C. Winter, captain of the R/V *Neeskay*, and D. Edgington, Great Lakes Water Center, University of Wisconsin-Milwaukee, for their assistance in acquisition of the 1993 box core. We thank P. Simpson and L. Minc, Phoenix Memorial Laboratory, University of Michigan, for neutron activation analysis of samples. We gratefully acknowledge M. Brake and R. Rood, Cooperative Institute for Limnology and Ecosystems Research, University of Michigan, and R. Rossmann, Large Lakes Research Station, US Environmental Protection Agency, for their diverse and important contributions to elemental and radiometric analysis, quality assurance, and data management. We thank J. Zanglin, US Army Corps of Engineers, for providing summary historical information on the Sault Locks. The development of this manuscript was aided by a Natural Sciences and Engineering Research Council of Canada grant to E.D. Reavie and funding from the State of Minnesota for the Natural Resources Research Institute, Ely, Minnesota. Comments from J.P. Smol helped to improve this paper. This is contribution No. 1347 for Great Lakes Environmental Research Laboratory and contribution No. 382 for the Center for Water and the Environment at the Natural Resources Research Institute.

## References

- Alfassi, Z.B. 1998. Instrumental multi-element chemical analysis. Kluwer Academic Publishers, Dordrecht.
- American Society of Mechanical Engineers. 1981. National historic mechanical engineering landmark: Michigan – Lake Superior Hydro-Power Plant, 1918. American Society of Mechanical Engineers, New York.
- Anderson, J.M. 1976. An ignition method for determination of total phosphorus in lake sediments. *Water Res.* **10**: 329–331.
- Appleby, P.G., and Oldfield, F. 1992. Application of  $^{210}\text{Pb}$  to sedimentation studies. In *Uranium-series disequilibrium: applications to earth, marine and environmental sciences*. 2nd ed. Edited by M. Ivanovich and R.S. Hrenon. Clarendon, Oxford. pp. 731–778.
- Battarbee, R.W. 1986. Diatom analysis. In *Handbook of Holocene palaeoecology and palaeohydrology*. Edited by B.E. Berglund. John Wiley & Sons Inc., New York. pp. 527–570.
- Bayliss. 2000. Sault Ste. Marie timeline and history. Bayliss Public Library, Sault Saint Marie, Mich.
- Bennett, K.D. 1996. Determination of the number of zones in a biostratigraphical sequence. *New Phytol.* **132**: 155–170.
- Bennett, K.D. 2002. Documentation for psimpoll 4.10 and pscomb 1.03. Quaternary Geology, Department of Earth Sciences, Uppsala University, Uppsala, Sweden.
- Burt, A.J., McKee, P.M., Hart, D.R., and Kauss, P.B. 1991. Effects of pollution on benthic invertebrate communities of the St. Marys River, 1985. *Hydrobiologia*, **219**: 63–81.
- Camburn, K.E., Kingston, J.C., and Charles, D.F. 1984–1986. PIRLA diatom iconograph. PIRLA Unpublished Report Series No. 3. Indiana University, Bloomington, Ind.
- Carignan, R., Lorrain, S., and Lum, K.R. 1994. A 50-year record of pollution by nutrients, trace metals and organic chemicals in the St. Lawrence River. *Can. J. Fish. Aquat. Sci.* **51**: 1088–1100.
- Carney, H.J. 1982. Algal dynamics and trophic interactions in the recent history of Frains Lake, Michigan. *Ecology*, **63**: 1814–1826.
- Carter, M.W., and Moghissi, A.A. 1977. Three decades of nuclear testing. *Health Phys.* **33**: 55–71.
- Comans, R.N.J., and Hockley, D. 1992. Kinetics of cesium sorption on illite. *Geochim. Cosmochim. Acta*, **56**: 1157–1164.
- Cumming, B.F., Wilson, S.E., Hall, R.I., and Smol, J.P. 1995. Diatoms from British Columbia (Canada) lakes and their relationship to salinity, nutrients, and other limnological variables. *Bibliotheca Diatomologica*, Band 31. J. Cramer Publishing Company, Berlin.
- Dams, R., and Robbins, J.A. 1970. Nondestructive activation analysis of environmental samples. Special Report 48. Great Lakes Research Division, Institute of Science and Technology, University of Michigan, Ann Arbor, Mich.
- Dixit, S.S., Smol, J.P., Charles, D.F., Hughes, R.M., Paulsen, S.G., and Collins, G.B. 1999. Assessing water quality changes in the lakes of the northern United States using sediment diatoms. *Can. J. Fish. Aquat. Sci.* **56**: 131–152.
- Evans, D.W., Albert, J.J., and Clark, R.A., III. 1983. Reversible ion-exchange fixation of  $^{137}\text{Cs}$  leading to mobilization from reservoir sediments. *Geochim. Cosmochim. Acta*, **47**: 1041–1049.
- Flanagan, F.J. 1973. 1972 values for international geochemical reference samples. *Geochim. Cosmochim. Acta*, **37**: 1189–1200.
- Flanagan, F.J. 1974. Reference samples for the earth sciences. *Geochim. Cosmochim. Acta*, **38**: 1731–1744.
- Flynn, W.W. 1968. The determination of low levels of polonium-210 in environmental samples. *Anal. Chem. Acta*, **43**: 221–227.
- Goldberg, E.D. 1993. Geochronology with  $^{210}\text{Pb}$ . In *Symposium on Radioactive Dating*, Athens, November 1992. International Atomic Energy Agency, Vienna. pp. 122–130.
- Govindaraju, K. 1994. 1994 Compilation of working values and descriptions for 383 geostandards. *Geostand. Newsl.* **18**: 1–158.
- Hamdy, Y., Kinkhead, J.D., and Griffiths, M. 1978. St. Marys River water quality investigations, 1973–1974. Ontario Ministry of the Environment, Toronto, Ont.
- Hartig, J.H. 1987. Factors contributing to development of *Fragilaria crotonensis* Kitton pulses in Pigeon Bay waters of western Lake Erie. *J. Gt. Lakes Res.* **13**: 65–77.
- Hesselberg, R.J., and Hamdy, Y. 1987. Current and historical contamination of sediment in the St. Mary's River, 1987. Michigan Department of Natural Resources, Lansing, Mich.
- Hill, M.O., and Gauch, H.G. 1980. Detrended correspondence analysis, an improved ordination technique. *Vegetatio*, **42**: 47–58.
- International Joint Commission. 1951. Report of the International Joint Commission, United States and Canada, on the pollution of boundary waters. Washington, D.C., and Ottawa, Ont.
- International Joint Commission. 1997. 1996–1997 binational progress report on protection of Great Lakes water quality. International Joint Commission, Windsor, Ont.

- Karamanski, T.J. 1989. Deep woods frontier: a history of logging in northern Michigan. Wayne State University Press, Detroit, Mich.
- Kauss, P.B. 1991. Biota of the St. Mary's River: habitat evaluation and environmental assessment. *Hydrobiologia*, **219**: 1–35.
- Kenaga, D. 1979. Chromium in the St. Mary's River in the vicinity of the old North Western Leather Company at Sault Ste. Marie, Michigan. Michigan Department of Natural Resources, Lansing, Mich.
- Kerfoot, W.C., Robbins, J.A., and Weider, L.J. 1999. A new approach to historical reconstruction: combining descriptive and experimental paleolimnology. *Limnol. Oceanogr.* **44**: 1232–1247.
- Krammer, K., and Lange-Bertalot, H. 1986–1991. *Bacillariophyceae*. In *Süßwasserflora von Mitteleuropa 2/1–4*. Edited by H. Ettl, J. Gerloff, H. Hyenig, and D. Mollenhauer. Fischer, Stuttgart.
- Krause, G.L., Schelske, C.L., and Davis, C.O. 1983. Comparison of three wet-alkaline methods for digestion of biogenic silica in water. *Freshw. Biol.* **13**: 73–81.
- Liston, C.R., McNabb, C.D., Brazo, D., Bohr, J., Craig, J., Duffy, W., Fleischer, G., Knoecklein, G., Koehler, F., Ligman, R., O'Neal, R., Siami, M., and Roettger, P. 1986. Limnological and fisheries studies in relation to proposed extension of the navigation season, 1982 and 1983. U.S. Fish Wildl. Serv. Publ. FWS/OBS-80/62.3.
- Michigan Karst Conservancy. 2003. Presenting Fiborn Quarry's history. Michigan Karst Conservancy, Ann Arbor, Mich.
- Moss, B., Madgwick, J., and Phillips, G. 1996. A guide to the restoration of nutrient-enriched shallow lakes. Environment Agency, Broads Authority, Norfolk, UK.
- Murphy, J.R., and Riley, J.P. 1962. A modified single solution method for the determination of phosphate in natural waters. *Anal. Chim. Acta*, **27**: 21–36.
- Newton, S. 1976. Mackinac Island and Sault Ste. Marie. Pictorial and legendary. Black Letter Press, Grand Rapids, Mich.
- Nichols, S.J., Manny, B.A., Schloesser, D.W., and Edsall, T.A. 1991. Heavy metal contamination of sediments in the Upper Connecting Channels of the Great Lakes. *Hydrobiologia*, **219**: 307–315.
- Northern Michigan University. 2003. A chronology of lake navigation. Northern Michigan University, Marquette, Mich. [online]. Available from <http://www.nmu.edu/upstudies/UPinfo/UPMarit/CHRONO.htm> [accessed January 2003; updated November 1999].
- Patrick, R., and Reimer, C.W. 1966. The diatoms of the United States exclusive of Alaska and Hawaii. Monograph 13. Vol. 2. Part 1. Sutter House, Lititz, Pa.
- Press, W.H., Flannery, B.P., Teukosky, S.A., and Vetterling, W.T. 1989. Numerical recipes: the art of scientific computing (FORTRAN version). Cambridge University Press, Cambridge, UK.
- Reavie, E.D., and Smol, J.P. 1998. Freshwater diatoms from the St. Lawrence River. *Bibliotheca Diatomologica*, Band 41. J. Cramer Publishing Company, Berlin.
- Reavie, E.D., Smol, J.P., and Hall, R.I. 1995. An expanded weighted-averaging model for inferring past total phosphorus concentrations from diatom assemblages in eutrophic British Columbia (Canada) lakes. *J. Paleolimnol.* **14**: 49–67.
- Reavie, E.D., Smol, J.P., Carignan, R., and Lorrain, S. 1998. Diatom paleolimnology of two fluvial lakes in the St. Lawrence River: a reconstruction of environmental changes during the last century. *J. Phycol.* **34**: 446–456.
- Ritchie, J.C., and Ritchie, C.A. 2003. Bibliography of publications of <sup>137</sup>Cs studies related to erosion and sediment deposition. USDA-ARS, Hydrology and Remote Sensing Laboratory, Beltsville, Md. Occas. Pap. HRSL-2003-02.
- Robbins, J.A. 1978. Geochemical and geophysical applications of radioactive lead. In *Biogeochemistry of lead in the environment*. Edited by J.O. Nriagu. Elsevier/North-Holland Biomedical Press, Amsterdam. pp. 285–383.
- Robbins, J.A. 1985a. Great Lakes regional fallout source functions. US Department of Commerce, National Oceanic and Atmospheric Administration, Environmental Research Laboratories, Ann Arbor, Mich. Tech. Memo. ERL-GLERL-56.
- Robbins, J.A. 1985b. The coupled-lakes model for estimating the long-term response of the Great Lakes to time-dependent loadings of particle-associated contaminants. US Department of Commerce, National Oceanic and Atmospheric Administration, Environmental Research Laboratories, Ann Arbor, Mich. Tech. Memo. ERL-GLERL-57.
- Robbins, J.A., and Herche, L.R. 1993. Models and uncertainty in <sup>210</sup>Pb dating of sediments. *Verh. Int. Ver. Limnol.* **25**: 217–222.
- Robbins, J.A., Holmes, C., Halley, R., Bothner, M., Shinn, E., Graney, J., Keeler, G., tenBrink, M., Orlandini, K.A., and Rudnick, D. 2000. Time-averaged fluxes of lead and fallout radionuclides to sediments in Florida Bay, J. *Geophys. Res.* **105**: 28805–28821.
- Robbins, J.A., Edgington, D.N., Eadie, B.J., Meyer, S.L., Morehead, N.R., Rood, R.W., Szmania, D.C., and Taylor, E.J. 2004. Lake Michigan sediment cores (1992–1996): radionuclide profiles, summary data and optimized model based state variable values. National Technical Information Service, Springfield, Va. NOAA Data Rep.
- Rossmann, R. 1995. Trace element concentrations in 1988 Saginaw Bay sediments: comparison with historical data. In *The Lake Huron ecosystem: ecology, fisheries and the management*. Ecovision World Monograph Series. Edited by M. Munawar, T. Edsall, and J. Leach. S.P.B. Academic Publishing, Amsterdam. pp. 343–364.
- Scheffer, M.S., Hosper, H., Meijer, M-L., Moss, B., and Jeppesen, E. 1993. Alternative equilibria in shallow lakes. *Trends Ecol. Evol.* **8**: 275–279.
- Schelske, C.L. 1984. Comment on small particles of amorphous silica in the nepheloid layer. *J. Gt. Lakes Res.* **10**: 94–95.
- Schelske, C.L. 1991. Historical nutrient enrichment of Lake Ontario: paleolimnological evidence. *Can. J. Fish. Aquat. Sci.* **48**: 1529–1538.
- Schelske, C.L., and Hodell, D.A. 1995. Using carbon isotopes of bulk sedimentary organic matter to reconstruct the history of nutrient loading and eutrophication in Lake Erie. *Limnol. Oceanogr.* **40**: 918–929.
- Schelske, C.L., Stoermer, E.F., Conley, D.J., Robbins, J.A., and Glover, R.M. 1983. Early eutrophication in the lower Great Lakes: new evidence from biogenic silica in sediments. *Nature (London)*, **222**: 320–322.
- Schelske, C.L., Stoermer, E.F., Fahnenstiel, G.L., and Haibach, M. 1986. Phosphorus enrichment, silica utilization and silica depletion in the Great Lakes. *Can. J. Fish. Aquat. Sci.* **43**: 407–415.
- Smith, J.N. 2001. Why should we believe <sup>210</sup>Pb sediment geochronologies? *J. Environ. Radioact.* **55**: 121–123.
- Stevenson, R.J., Lowe, R.L., and Bothwell, M.L. 1996. *Algal ecology — freshwater benthic ecosystems*. Academic Press, San Diego, Calif.
- Stoermer, E.F. 1980. Characteristics of benthic algal communities in the upper Great Lakes. US Environmental Protection Agency, Environmental Research Laboratory, Duluth, Minn. Ecol. Res. Ser. EPA 600/3-80-073.
- Stoermer, E.F., and Ladewski, T.B. 1976. Apparent optimal temperatures for the occurrence of some common phytoplankton species in southern Lake Michigan. *Univ. Mich. Gt. Lakes Res. Div. Spec. Rep. No. 18*.
- Stoermer, E.F., Wolin, J.A., Schelske, C.L., and Conley, D.J. 1985a. An assessment of ecological changes during the recent history of

- Lake Ontario based on siliceous microfossils preserved in the sediments. *J. Phycol.* **21**: 257–276.
- Stoermer, E.F., Kociolek, J.P., Schelske, C.L., and Conley, D.J. 1985*b*. Siliceous microfossil succession in the recent history of Lake Superior. *Proc. Acad. Nat. Sci. Phila.* **137**: 106–118.
- Stoermer, E.F., Emmert, G., and Schelske, C.L. 1989. Morphological variation of *Stephanodiscus niagarae* (Bacillariophyta) in a Lake Ontario sediment core. *J. Paleolimnol.* **2**: 227–236.
- Stoermer, E.F., Wolin, J.A., Schelske, C.L., and Conley, D.J. 1990. Siliceous microfossil succession in Lake Michigan. *Limnol. Oceanogr.* **35**: 959–967.
- Stoermer, E.F., Wolin, J.A., and Schelske, C.L. 1993. Paleolimnological comparison of the Laurentian Great Lakes based on diatoms. *Limnol. Oceanogr.* **38**: 1311–1316.
- Stoermer, E.F., Emmert, G., Julius, M.L., and Schelske, C.L. 1996. Paleolimnologic evidence of rapid recent change in Lake Erie's trophic status. *Can. J. Fish. Aquat. Sci.* **53**: 1451–1458.
- Tannery. 1983. The Tannery reunion story, Tannery Employees Reunion, August 19–20, 1983, Walker Cisler Center, Lake Superior State College, Sault Saint Marie, Mich. Bayliss Public Library, Sault Saint Marie, Mich.
- Tenzer, G.E., Meyers, P.A., Robbins, J.A., Eadie, B.J., Morehead, N.R., and Lansing, M.B. 1999. Sedimentary organic matter record of recent environmental changes in the St. Marys River ecosystem, Michigan–Ontario border. *Org. Geochem.* **30**: 133–146.
- ter Braak, C.J.F. 1995. Ordination. *In* Data analysis in community ecology. *Edited by* R.H. Jongman, C.J.F. ter Braak, and O.F.T. van Tongeren. Pudoc, Wageningen, Netherlands. pp. 91–173.
- ter Braak, C.J.F., and Šmilauer, P. 2002. CANOCO reference manual and CanoDraw for Windows user's guide: software for canonical community ordination (version 4.5). Microcomputer Power, Ithaca, N.Y.
- Thayer, V.L., Johnson, T.C., and Schrader, H.J. 1983*a*. Distribution of diatoms in Lake Superior sediments. *J. Gt. Lakes Res.* **9**: 497–507.
- Thayer, V.L., Johnson, T.C., and Schrader, H.J. 1983*b*. A preliminary study of recent diatom assemblages in Lake Superior sediments. *J. Gt. Lakes Res.* **9**: 508–516.
- Treasury. 1929–1957. Annual financial reports of the Northwestern Leather Co. to the Michigan Department of State, Michigan Corporate Division, Lansing, Mich. Bayliss Public Library, Sault Saint Marie, Mich.
- Upper Great Lakes Connecting Channels Study. 1989. Vol. II. Final report of the Upper Great Lakes Connecting Channels Study. Environment Canada, U.S. Environmental Protection Agency, Michigan Department of Natural Resources, Ontario Ministry of the Environment, National Oceanographic and Atmospheric Administration, U.S. Fish and Wildlife Service, U.S. Army Corps of Engineers, and Detroit Water and Sewerage Department, Detroit, Mich.
- Van Dam, H., Mertens, A., and Sinkeldam, J. 1994. A coded checklist and ecological indicator values of freshwater diatoms from the Netherlands. *Neth. J. Aquat. Ecol.* **28**: 117–133.
- Wolin, J.A., Stoermer, E.F., Schelske, C.L., and Conley, D.J. 1988. Siliceous microfossil succession in recent Lake Huron sediments. *Arch. Hydrobiol.* **114**: 175–198.
- Wolin, J.A., Stoermer, E.F., and Schelske, C.L. 1991. Recent changes in Lake Ontario 1981–1987: microfossil evidence of phosphorus reduction. *J. Gt. Lakes Res.* **17**: 229–240.